2016

A Simulation and Experimental Study of Active Disturbance Rejection for Industrial Pressure Control

Xiaoxu Li

A SIMULATION AND EXPERIMENTAL STUDY OF ACTIVE DISTURBANCE REJECTION FOR INDUSTRIAL PRESSURE CONTROL

XIAOXU LI

Bachelor of Science in Network Engineering

City Institute Dalian University of Technology, Dalian, China

July 2010

submitted in partial fulfillment of requirements for the degree

MASTER OF SCIENCE IN ELECTRICAL ENGINEERING

at the

CLEVELAND STATE UNIVERSITY

December 2016

We hereby approve this thesis for

Xiaoxu Li

Candidate for the Master of Science in Electrical Engineering
degree for the Department of Electrical Engineering and Computer Science
and the CLEVELAND STATE UNIVERSITY
College of Graduate Studies

Thesis Chairperson, Zhiqiang Gao, Ph.D.

Department & Date

Lili Dong, Ph.D.

Department & Date

Hongxing Ye, Ph.D.

Department & Date

Student's Date of Defense: December 7, 2016

ACKNOWLEDGMENTS

I would like to express my sincere gratitude to my thesis advisor Dr. Zhiqiang Gao for his unfailing support to my graduate studies, for the caring, understanding, patience and friendship that he always extended to me. Without Dr. Gao's valuable suggestions, encouragement, and thoughtful guidance it would not be possible to conduct and complete this research project. I would like to thank him for his contribution to my professional advancements.

Special appreciations are due to Dr. Lili Dong and Dr. Hongxing Ye for their precious time, help, advice and for the learning opportunities that they provide to me. I also would like to thank Dr. Sally Shao for her advice, suggestions and her help to revise this thesis.

I would like to express my deep thanks to Mr. Gregg Calhoun, who spent a lot of time on helping me troubleshooting the experiment equipment. He had been always willing to help and supported me greatly. I am grateful to my lab mates Qinling Zheng, Han Zhang, Lei Wang and Yu Hu, and our lab visitors Rafal Madonski, Mario Ramirez-Neria and Qirui Zhang. Special thanks to Qinling Zheng for our stimulating discussions.

My sincere thanks also goes to my manager at work Mr. Peter Ehler, my team lead Mr. Scott Wallace, Maria Baker, Mr. Ken Lowenthal and all my colleagues at CSA Group, for their understanding and support throughout the writing of this thesis.

Finally, I wish to express my profound gratitude to my parents, my grandparents and my fiance Hui Xin for their love, unlimited support and encouragement throughout my years of studies, which help me through the processes of conducting research and finishing this thesis. It would not have been possible without them.

A SIMULATION AND EXPERIMENTAL STUDY OF ACTIVE DISTURBANCE REJECTION FOR INDUSTRIAL PRESSURE CONTROL

XIAOXU LI

ABSTRACT

The quality of control loop is very important in hydraulic machineries, where pressure must be accurately regulated in the presence of various disturbances. Proportional-Integral-Derivative (PID) control has dominated the industry for a long time and it is by far the most popular general purpose controller for pressure control. The purpose of this study is to conduct a simulation and experimental study comparing PID with an emerging new technology, namely active disturbance rejection control (ADRC). For the purpose of this study, an experimental testbed similar to those used in industry settings is used; its mathematic model is derived and used in the simulation study. A linearized model is also derived for the purpose of PID tuning, where various methods such as the standard Ziegler-Nichols method, the pole-placement and the trial-and-error method are tested. As for the tuning of ADRC, a method is proposed to determine the critical gain parameter, which is the only plant parameter needed. All the simulation and experimental tests are designed based on the practical scenarios, so that the controller tuning, the tracking performance, the disturbance rejection capability and the energy consumption can be studied meaningfully for future industrial applications. Initial results indicate that, with the same bandwidth, ADRC can be used in a wider range of set point tracking than PID. Furthermore, ADRC is easy to tune and has clear advantages over PID in terms of disturbance rejection and energy saving in all simulation and experiment results. In summary, results of this study indicates that ADRC, as a general purpose controller, is a viable solution for pressure control applications, and an alternative to PID.

TABLE OF CONTENTS

LIST OF FIGURES

LIST OF TABLES

CHAPTER I

INTRODUCTION

Automatic control plays an important role in all sectors of industry and PID as a general purpose controller has been dominant for over a hundred years, despite the rapid progress made in both hardware and software. Many mathematically elegant solutions have appeared in the literature and they can be readily implemented in the increasingly powerful industrial control platforms, but none of them has come close to threaten the dominance of PID. Of course PID is far from perfect as an engineering solution. On the contrary, the weaknesses of PID are rather obvious: it is implemented as a simple linear weighted sum of various forms of the tracking error, because of the hardware limitations that have long disappeared, leading to unnecessary performance bottleneck; the integral control action introduces phase lag and brings stability complications; and the derivative control makes the system sensitive to sensor noises. Such reality of "advanced control theory" and "backward" control practice has continued to drive researchers in the seeking the alternatives of PID. In this research, in the context of an industry pressure control problem, the search continues. The objective here is to find a new general purpose controller capable of replacing the PID. Learning from the lessons in the previous "advanced" control solutions, the emphasis in this

study has been put on the simplicity of controller tuning, the tracking performance, the disturbance rejection capability and the energy consumption.

1.1 Background

In this chapter, we begin with a review of the background of industrial control technology and its evolution. Control plays a vital and independent role in the engineering and sciences. Early inventions of automatic control can be traced back as far as the "South Pointing Chariot" [1] of China in 900 B.C. , shows in Fig.1.1. It is an ingenious solution to the problem of angle preservation, where the figure of the wooden figure on top of the chariot always points south, its starting direction, no matter how the chariot moves and turns. The design principle of this famous invention from ancient China escaped the grasp of human being for thousands of years and it is a vivid rebuke of the common notion that technology is invented from applications of theories. Similarly, control theory did not have anything to do with the invention of the flyball governor, which brought us the Industrial Revolution and modern life style. In fact, the further developments of control technology in the 19th and 20th centuries proceeded without much contribution of control theory, covering a wide spectrum of modern industry, from manufacturing to aerospace and aeronautics, and so on. A particular sector of industrial control is process control, with which this thesis is concerned.

Process control is an important part of automatic control that can improve safety, reduce environmental impacts, and optimize process operations by maintaining process variables near their desired values. In particular, maintaining process variables in a desired operating range is of the utmost importance in manufacturing products with a predictable composition and quality. The practical importance also makes process control a significant theoretical content in control education as well [3].

The vapor or gas pressure is one of the most common process variables subject to automatic control. It could be either as an end in itself or as a means of controlling a more complicated

Figure 1.1: South Pointing Chariot [2]

system. The pressure of a liquid which is not in contact with a gas or vapor is controlled continually as well, usually in hydraulic pump systems. In terms of the control problem, solids pressure is not easy to identify. However, changes in either tension or compression of solid construction materials such as steel are often suitable for measurement and for use as a step in the control of variables that are related to the strain in the material [4]. The pressure dynamic is treated as one of the most important topics in process control textbooks, such as [5–10]. Also, the pressure dynamic experiments are widely used to demonstrate the process control textbook theory [3].

Over the years, various control algorithms have been developed and applied for air pressure control, including sliding mode [11], adaptive control [12], predictive control [13], Fuzzy Logic control [14], etc. The particular control methodology used may cause significantly different per-

formance and it has its own range of applications. However, PID as the general purpose controller is by far the most widely used solution in pressure control systems.

It is estimated that over 90 percent of process control solutions is of the PID type [15]. A steam boiler system is one of the pressure control applications closely related to people's daily life. It is a complex industrial process, usually designed to work at high pressure in order to reduce their physical size. Boiler system is usually associated with significant nonlinearity, large transport delay, strong coupling among subsystems, and a lot of load disturbances. Like other pressure control systems, the current steam pressure control system is mainly dominated by traditional PID control [16, 17]. The fastest growing application of pressure control is automotive. The market of diesel engines has rapidly extended from commercial vehicles to passenger cars in the past decades. The diesel engine is a very complicated system and it is dominantly controlled by PID as well [18, 19]. Another key application of pressure control system is chemical reaction of the combustion system. The amount of combustible material going into the tank is controlled by the rate of air flow going into the tank. The rate of combustion reactions will be largely defined by the pressure building in the tank and is again controlled by PID [20].

The wide use of PID control in the field of pressure control gives rise to various tuning methods for it. The Ziegler-Nicholas (Z-N) [21] is probably the most well known and most commonly used method for tuning of PID controllers [22]. Although the tuning parameters give the good result at the operating point, it is limited in operating range [23–25]. In addition, there is no method of PID tuning that can be applied to all plants and a lot of time is wasted in tuning the PID parameters in practice. It also led to an enormous enormous literature on PID tuning method [26, 27]. It is shown that over 1000 rules for tuning proportional integral (PI) and PID have been proposed and the list is continuously growing [28–30].

The difficulty in PID tuning reflects a fundamental limitation in industrial control technology where the main problem to how to deal with the uncertainties simply, effectively and economically. The model-based modern control theory is illsuited for such challenge because of its insistence in

assuming that most, if not all, process dynamics is known beforehand. Even when such solutions are developed, they are often described in mathematical symbols most engineers wouldn't be able to understand and they are often too complex to implement or to tune by the users.

In response to the gap between control theory and practice, a handful of researchers went their own way in establishing an alternative framework to address the problems of industrial control, to different degrees of success. One such framework that has emerged as leading candidate to the PID framework is the so called active disturbance rejection control (ADRC), first proposed by J. Han [31–36]. It was based on the careful analysis of PID, both its strength and weaknesses, and the recognition that the problem of uncertainties and the problem of disturbance rejection are one and the same. In fact, a concept central in ADRC is the concept of total disturbance, which includes both the unknown dynamics and the external disturbances in the physical process. This allows the control design to be performed on an ideal model, such as the pure integral model, and treat all other dynamics as a part of total disturbance to be estimated in real time and canceled by the control signal.

ADRC was originally developed to address the weaknesses of PID with three main components: the tracking differentiator (TD), the nonlinear state feedback (NLSF) and the extended state observer (ESO) [37]. In particular, TD is designed to general smooth reference signal and its derivative; NLSF is a nonlinear version of the linear weighted sum of various forms of the tracking used in the PID; ESO is the mechanism to estimate the total disturbance. Conceived, developed and applied, ADRC proved to be a very effective control framework that systematically addressed the weakness of PID and the limitations of modern control theory.

ADRC was further simplified and streamlined by Z. Gao in 2003 [38], from which a new kind of industrial control technologies was born. This is made possible by replacing the nonlinear gains in the original ADRC with linear ones, thus giving a linear ADRC or LADRC. Over the last decade since it was proposed, LADRC has been widely tested and used in the research and practice: the test of ADRC on an industrial notion control platform was reported in [39]; an energy

saving, factory-validated disturbance decoupling control design for extrusion processes was seen in [40]; and some industry giants such as Texas Instruments and Freescale Semiconductor Inc. have replaced PID in their products with LADRC and made new digital control chips [28]. The readers are referred to [41–50] for more reports and articles regarding such developments.

Related to process control, LADRC has been applied, for instance, to the control of the air-fuel ratio of gasoline engine, which has large nonlinear uncertainties due to the unknown speed change, and fuel film dynamics [51, 52]. Combustion boiler is another example [53–55]. Furthermore, many simulations and experiments show the good performance on the systems with time-delay, vibration controlled by LADRC [56, 57]. These initial successes provided the initial motivation for this research in search of a general purpose controller for pressure control in industrial settings. To make our study realistic, an experimental testbed is first established, as described below.

1.2 Experimental Testbed

The comparison study will be performed in simulation and in hardware based on the air pressure and flow testbed at the CSU control laboratory. It mimics a standard industrial pressure and flow control installation, which was designed to provide students with hands-on experience on pressure and flow control. In this study, the focus is on the pressure control, as stated earlier. The snapshot of experimental testbed of pressure control system is shown in Fig.1.2. The service air (air source) is approximately 100 psig. The air passes through the pipeline into the pressure and flow system and it can be turned on and off using a hand valve. The airflow into the air tank is regulated using a pneumatic valve. A pressure transducer is installed in the tank and its output signal is captured by the encoder linked to PC through a data acquisition board. The PC functions as a controller using the Matlab/Simulink software package by which the control algorithm, whether it is PID or ADRC, is coded and executed.

The output from the controller changes the pneumatic valve opening by manipulating the cur-

rent in the current to pressure converter (I/P). The controller regulates the control valve opening for airflow to maintain the pressure inside the control tank. A flow meter is connected to the pneumatic valve to monitor the flow rate of the air. A back pressure regulator is installed in the tank to provide another way of pressure control. In this study, however, it is used as a disturbance generator to introduce leakage to the system.

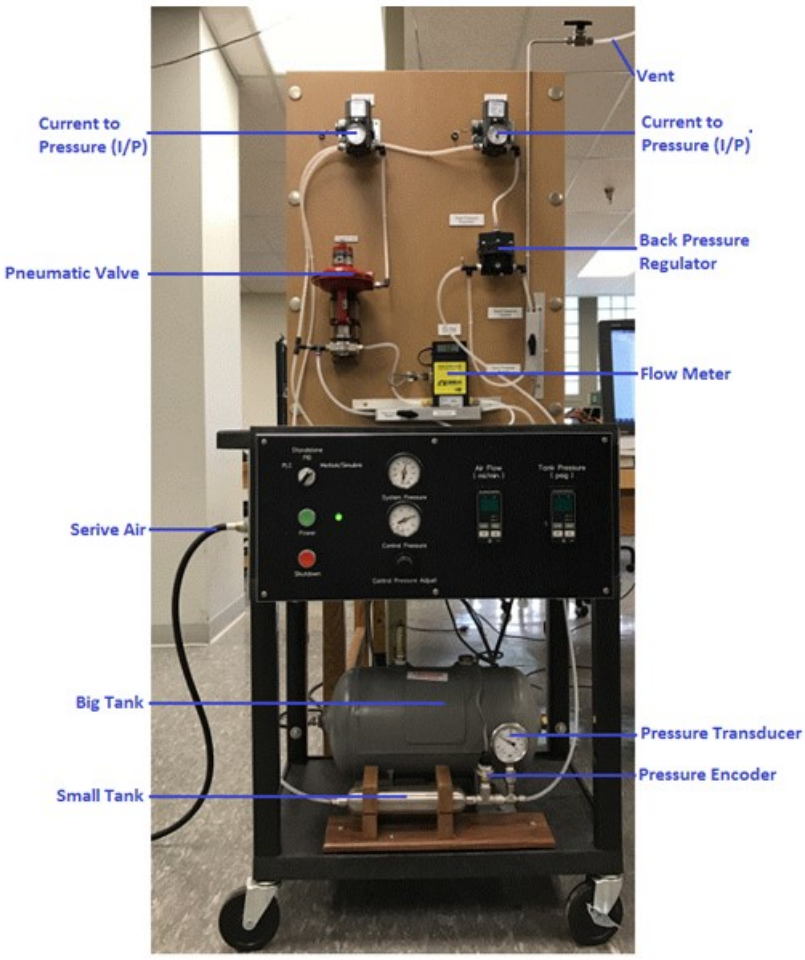

Figure 1.2: The Snapshot of Experimental Testbed

1.3 Thesis Organization

The thesis is organized as follows. The compressible and incompressible air models of pressure and flow system dynamics are built in Chapter 2. They will be used later on in the simulation study and in controller tuning. The comparison of the two models with the plant is described as well. A lot of efforts were spent to make the model output consisted with the test data, which proves to be quite challenging. As the prime candidates for pressure control, both PID and ADRC algorithms are introduced in Chapter 3, where the controller tuning issues are also addressed. The comparison study between PID and ADRC is carried out in simulation as shown in Chapter 4. The tracking performance is demonstrated first, follow by the load disturbance tests. In addition, the external disturbances are added to the simulation study to show disturbance rejection ability of each controller. The implementation and experiment results along with the comparisons of PID and ADRC in tracking performance, disturbance rejection capability and energy consumption in the real system are presented in Chapter 5. Finally, concluding remarks are given in Chapter 6 where the impact and significance of this work, as well as possible future work, are shown.

CHAPTER II

MODELING AND DYNAMICS

The subjects of this comparison study, PID and ADRC, as general purpose controllers for industrial applications are basically “model-free ”control algorithms in that neither of them requires detailed mathematical model of the process to be controller. But modeling presented in this chapter is nonetheless important because it helps us understand better the dynamics of the plant; it also helps us build a simulation model with high fidelity, which is important in the simulation study. The modeling effort also proves beneficial later on in controller tuning process for both PID and ADRC, although the latter needs much less information. The pressure control system used in this study mainly comprises of three components: pneumatic flow valve, air tank, and back pressure regulator. The air pressure dynamics based on the ideal gas law is described in Section 2.1; the incompressible and compressible models of the mass flow rate through the valve are derived in Section 2.2. Section 2.3 presents the actual incompressible and compressible flows based on the basic fluid mechanics laws. Finally, the adjusted plant models and the model validation are presented.

2.1 Pressure Dynamics

The tank is the main component of the entire system, where the air pressure obeys the ideal gas law:

$$pV = nRT \tag{2.1}$$

The descriptions of parameter in the ideal gas law are shown in Table. (2.1)

Table 2.1: Parameters of Ideal Gas Law

Parameters	**Descriptions**	**Units**
p	pressure	pascal
V	volume	m^3
n	number of moles of gas	mole
R	gas constant	J/(mole*K)
T	absolute temperature	K

Assuming adiabatic conditions (no heat or mass is transferred), a given amount of gas that undergoes a volumetric change will experience a related energy change:

$$dW = -pdV \tag{2.2}$$

where W is the energy. The energy change can be expressed for a corresponding temperature change as:

$$dW = nc_V dT \tag{2.3}$$

where c_V is the specific heat at constant volume. Solving p, in Eq. (2.1), and Eq. (2.2), we have

$$\frac{dV}{V} = -\frac{c_V}{R}\frac{dT}{T} \tag{2.4}$$

Integrating both sides of Eq. (2.4), we obtain

$$\ln\frac{V_2}{V_1} = -\frac{c_V}{R}\ln\frac{T_2}{T_1} \tag{2.5}$$

or,

$$\frac{T_2}{T_1} = (\frac{V_2}{V_1})^{-R/c_V} \tag{2.6}$$

c_p is the specific heat at constant pressure, the unit of c_V and c_p is $J/(mol*K)$, the relation between them is:

$$R = c_p - c_V \tag{2.7}$$

and the ratio between them is:

$$k = c_p/c_V \tag{2.8}$$

substituting Eq. (2.8) into Eq. (2.6), we have

$$\frac{T_2}{T_1} = (\frac{V_2}{V_1})^{1-k} \tag{2.9}$$

or,

$$TV^{k-1} = constant \tag{2.10}$$

Similarly, for the adiabatic, using Eq. (2.1),

$$\frac{T_2}{T_1} = (\frac{p_2}{p_1})^{(k-1)/k} \tag{2.11}$$

or,

$$Tp^{1-k} = constant \tag{2.12}$$

and,

$$\frac{p_2}{p_1} = (\frac{V_1}{V_2})^k \tag{2.13}$$

or,

$$pV^k = constant \tag{2.14}$$

comparing Eq. (2.14) with Eq. (2.2) for the isothermal case:

$$pV = constant \tag{2.15}$$

Assume that a gas is added into a constant volume tank with constant temperature, together with Eq. (2.2), we obtain:

$$\frac{dp}{dt} = \frac{dn}{dt} \cdot \frac{RT}{V} \tag{2.16}$$

Eq. (2.16) expresses that the changes rate of pressure is proportional to the net flow of the gas, the gas flow goes into the tank is measured in moles; proportional to the absolute temperature, and inversely proportional to the tank volume.

$$\frac{dn}{dt} = m_1 - m_2 \tag{2.17}$$

where m_1: mass flow into the tank $(mole/s)$, and m_2: mass flow out of the tank $(mole/s)$, Eq. (2.16) can be rewritten as:

$$\frac{dp}{dt} = \frac{RT}{V}(m_1 - m_2) \tag{2.18}$$

Thus, the pressure is characterized by an integration from the mass flow to pressure.

2.2 Valve Mass Flow

The pressure in the tank can be controlled by operating the mass flow rate of either the feed stream or the output stream. The characteristics of the final control valve determine whether the pressure control system will have difficulties in terms of dynamics.

2.2.1 Incompressible Model

Assuming completely isolated condition, ignore friction and inertial effects in the flow, and the fluid is incompressible, by Bernoulli's law:

$$P_1 + \rho g h_1 + \frac{1}{2}\rho V_1^2 = P_2 + \rho g h_2 + \frac{1}{2}\rho V_2^2 \tag{2.19}$$

Ignore the air heights and no input volume, Eq. (2.19) can be rewritten as

$$P_1 - P_2 - \frac{1}{2}\rho V_2^2 = 0 \tag{2.20}$$

Thus, the volume of the air tank is derived:

$$V = \sqrt{\frac{2(P_1 - P_2)}{\rho}} \tag{2.21}$$

and

$$m = \rho V A \tag{2.22}$$

so,

$$m(t) = c_d . A(t) . \sqrt{2\rho} . \sqrt{p_{in}(t) - p_{out}(t)} \tag{2.23}$$

where the following definitions have been used:

Table 2.2: Parameters of Incompressible Model

Parameters	**Descriptions**	**Units**
m	mass flow through the valve	kg/s
c_d	discharge coefficient	N/A
A	cross-section of the valve	m^2
ρ	density of the fluid, assumed to be constant	kg/m^3
p_{in}	pressure upstream of the valve	Pascal
p_{out}	pressure downstream of the valve	Pascal

The discharge coefficient can be a variable, changing with valve position; however, an average value for C_d of 0.62 is often used to simplify calculations of leaving area A to change with valve position.

2.2.2 Compressible Model

For compressible fluids, the most important and versatile flow control block are the isothermal orifice. The process of deriving the mass flow equation can be founded in the book: Introduction to Modeling and Control of Internal Combustion Engine Systems [58], Section 2.3 Air System.Assume that the temperature is constant; no losses occur in the accelerating part up to the narrowest point. The flow is fully turbulent and all of the kinetic energy gained in the first

part is dissipated into thermal energy. After the narrowest point, no pressure recuperation takes place [58]. Using the theory of the thermodynamic for isentropic fluid the following equation of compressible model can be obtained:

$$m(t) = c_d.A(t).\frac{p_{in}(t)}{\sqrt{R.T}}.\Psi(\frac{p_{in}(t)}{p_{out}(t)}) \tag{2.24}$$

where the flow function $\Psi(\frac{p_{in}(t)}{p_{out}(t)})$ is defined by

$$\Psi(\frac{p_{in}(t)}{p_{out}(t)}) = \begin{cases} \frac{1}{\sqrt{2}} & \text{for} \quad p_{out} < \frac{1}{2}p_{in} \\ \sqrt{\frac{2p_{out}}{p_{in}}.[1-\frac{p_{out}}{p_{in}}]} & \text{for} \quad p_{out} \geq \frac{1}{2}p_{in} \end{cases} \tag{2.25}$$

2.3 Modeling

Fig.2.1 shows the diagram of the air pressure and flow system. Mass flow through the pneumatic valve and air pressure in the tank are the mainly modeling parts. The backpressure regulator is used to introduce disturbance to test the controller performance. For modeling, the regulator is closed which means the output flow equal to zero.

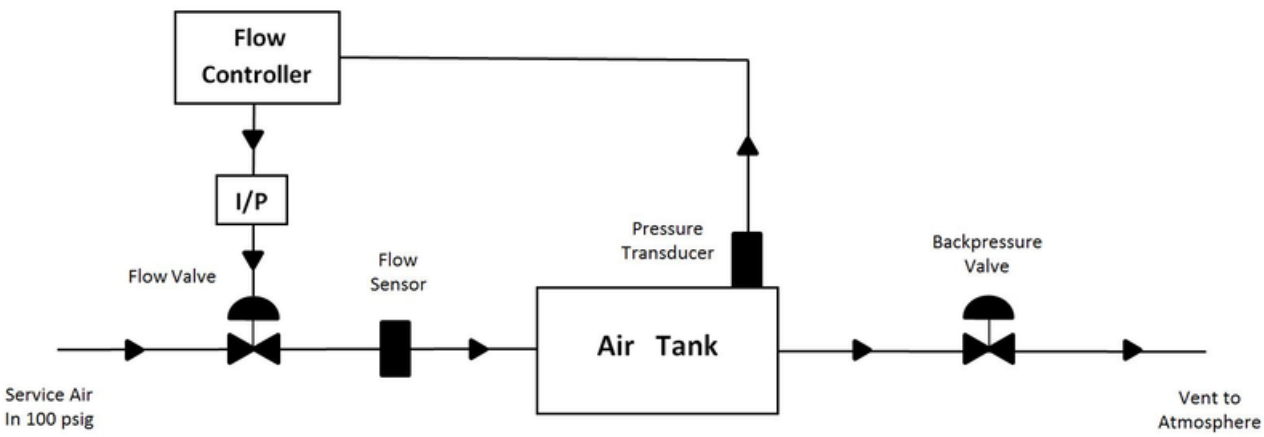

Figure 2.1: Experimental Testbed Diagram

thus, Eq. (2.18) can be rewritten as:

$$\frac{dp}{dt} = (\frac{RT}{V}).m_{in}(t) \tag{2.26}$$

Substituting Eq. (2.23) into Eq. (2.26) gives the incompressible air pressure model:

$$\frac{d}{dt}p(t) = (\frac{RT}{V}).[c_d.A(t).\sqrt{2\rho}.\sqrt{p_{in}(t) - p_{out}(t)}] \tag{2.27}$$

And substituting Eq. (2.24) into Eq. (2.26) gives the compressible air pressure model:

$$\frac{d}{dt}p(t) = \begin{cases} (\frac{RT}{V}).[c_d.A(t).\frac{p_{in}(t)}{\sqrt{R.T}}].\frac{1}{\sqrt{2}}; & \text{for} \quad p_{out} < \frac{1}{2}p_{in} \\ (\frac{RT}{V}).[c_d.A(t).\frac{p_{in}(t)}{\sqrt{R.T}}].\sqrt{\frac{2p_{out}}{p_{in}}.[1 - \frac{p_{out}}{p_{in}}]} & \text{for} \quad p_{out} \geq \frac{1}{2}p_{in} \end{cases} \tag{2.28}$$

The relation between cross-section of the valve and a unit control signal is:

$$A(t) = [\frac{u-1}{4}] \tag{2.29}$$

where u is the flow control signal in voltage, from 1 to 5 volts. The parameters of the plant are shown below in Table. (2.3):

Table 2.3: Parameters of Actual Plant

Parameters	**Value**	**Units**
R	287.05	$J/(kgK)$
T	20	Celsius
V	0.00042	m^3
C_d	0.62	N/A
p_{in}	735670.6	Pascal
A	2×10^{-6}	m^2

Substituting the parameters in Table. (2.3) into Eq. (2.27) and Eq. (2.28), respectively, we obtain the compressible pressure model versus incompressible pressure model in Fig.2.2. The response of the corresponding compressible and incompressible mass flow are shown in Fig.2.3.

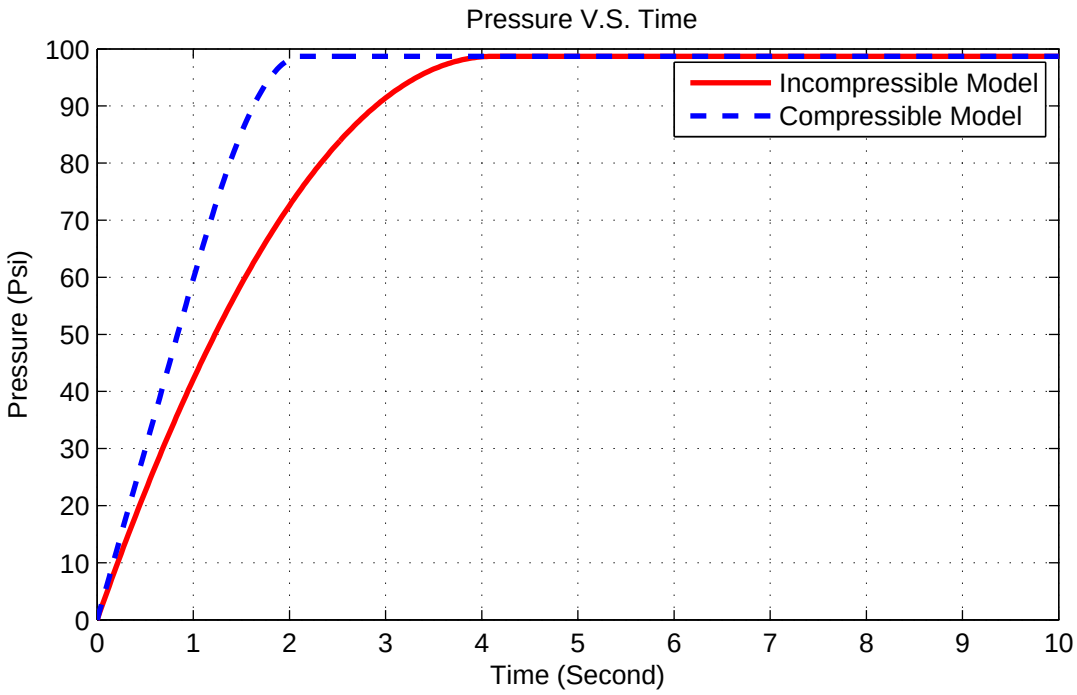

Figure 2.2: Compressible VS. Incompressible Pressure

The difference between the compressible pressure performance and the incompressible pressure performance is not significant except the settling time. However, the difference between compressible flow and incompressible flow is remarkable.

For the incompressible flow, the model is based on the Bernoulli's law, which is the classic orifice or valve equation, valid for steady, incompressible flow. For compressible flow, the model describes the difference between high and low pressure drop flow conditions. In high pressure drop flow, when outlet pressure P_{out} is smaller than half of inlet pressure P_{in}, the air leaves the orifice at the velocity of sound. The air cannot exceed the velocity of sound, therefore, this becomes the maximum flow rate. High pressure drop flow only depends on inlet pressure and temperature,

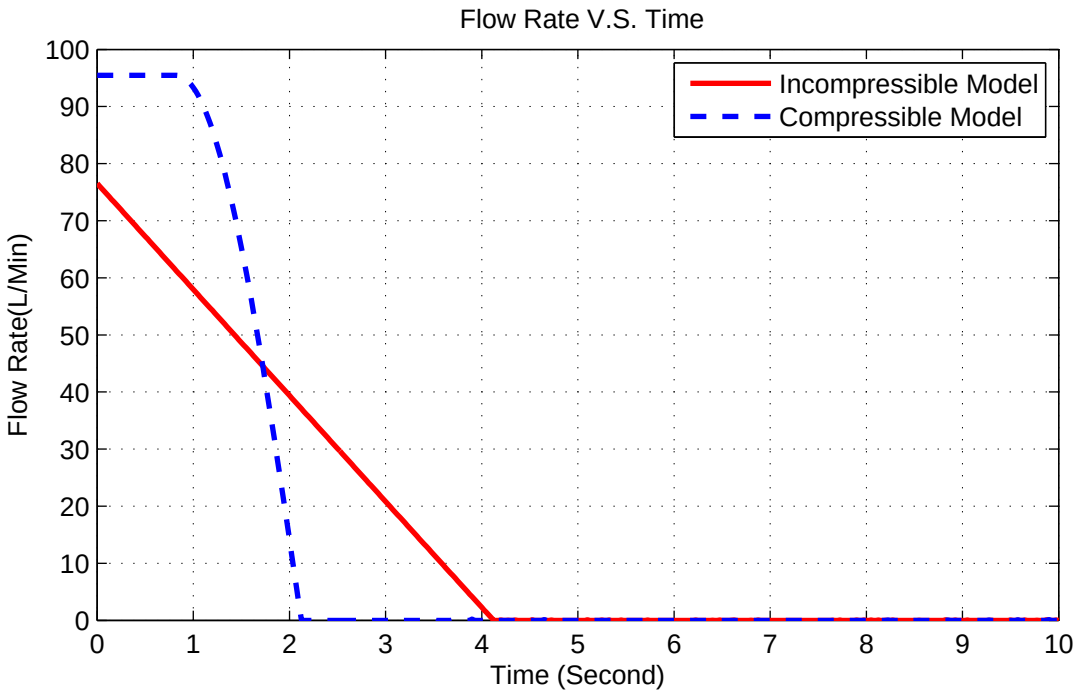

Figure 2.3: Compressible VS. Incompressible Flow

valve flow coefficient, and specific gravity of the gas. When outlet pressure P_{out} is greater than half of inlet pressure P_{in} which is low pressure drop flow, outlet pressure restricts flow through the orifice: as outlet pressure decreases, flow increases, so does the velocity of the air leaving the orifice.

2.4 Model Validation

By comparing the performances of the compressible and incompressible models with the real system, the settling time has approximately 100 times differences. The mass flow Eq. (2.23) and Eq. (2.24) are used to present the fundamental stage flow characteristics of a classic proportional valve. However, the valve installed on the plant is a pneumatic proportional valve. The behavior of the pneumatic valve is highly nonlinear and complicated. The accurate mathematical model of pneumatic valve is not concerned in this research. Thus, an adjusted gain k is added to make the

models match the actual plant. $k = 0.018, 0.013$ are obtained by the experiments for the incompressible and compressible model respectively. Moreover, the slightly leakage of the real system is shown during the experiments by adding the output flow $m_{out} = 0.023$ L/Min. After the adjustments, the mathematic models versus actual plant tracking are showed in Fig.2.4 and Fig.2.5. The shadow part in the actual plant of flow shown in Fig.2.5 is the noise producted by the flow sensor.

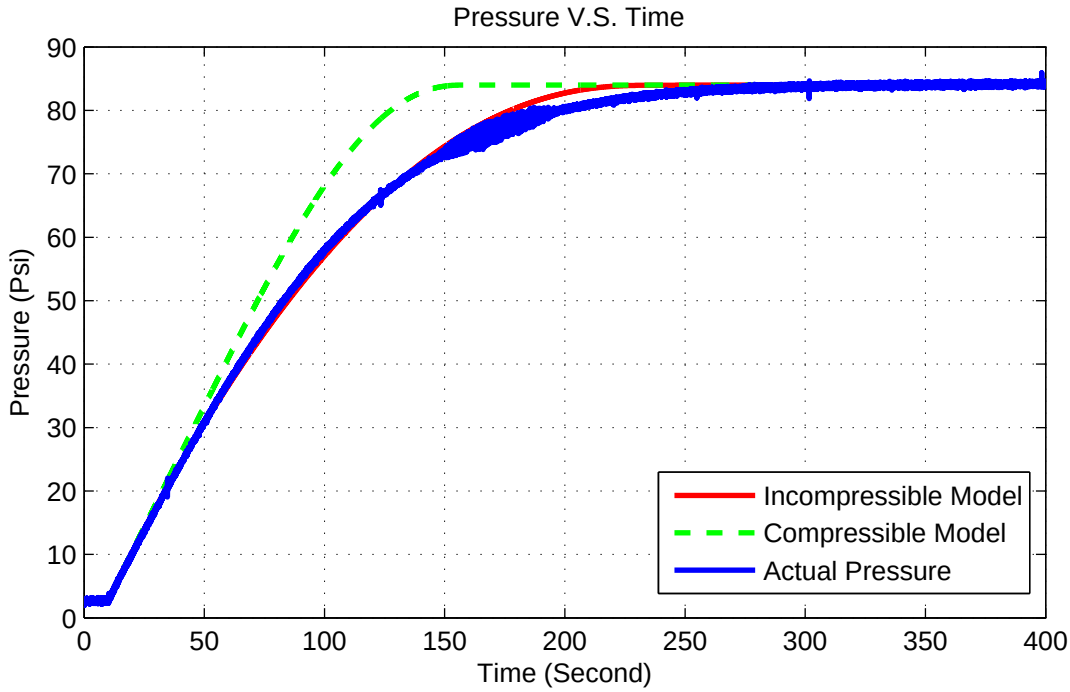

Figure 2.4: Mathematic Model VS. Actual Plant in Pressure

From Fig.2.5, the characteristic of the incompressible flow model is closer to the real system, that is because the compressible model treats the high pressure drop air flow as sonic velocity. In practice, the real system has few temperature changes, and the velocity is much slower than the velocity of sound. In order to show the incompressible mass flow model fits the actual plant better than the other one, root-mean-square (RMSD) deviation is plotted as Fig.2.6. According to the RMSD figure, for the incompressible model, Fig.2.5 is choosen to be used as the plant mathematic model.

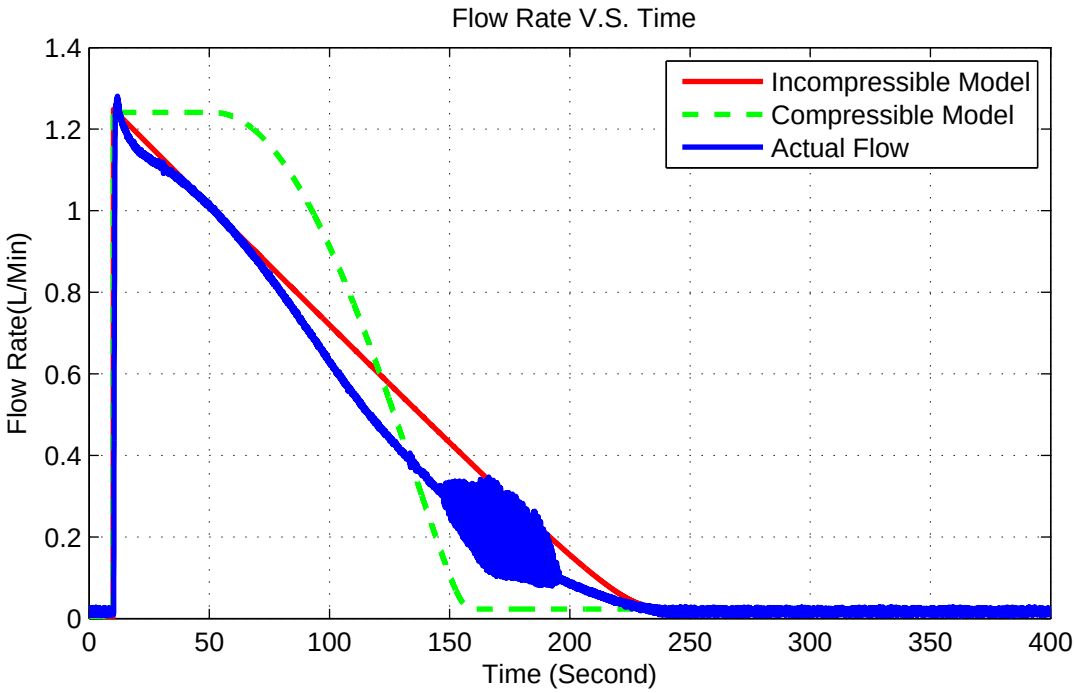

Figure 2.5: Mathematic Model VS. Actual Plant in Flow

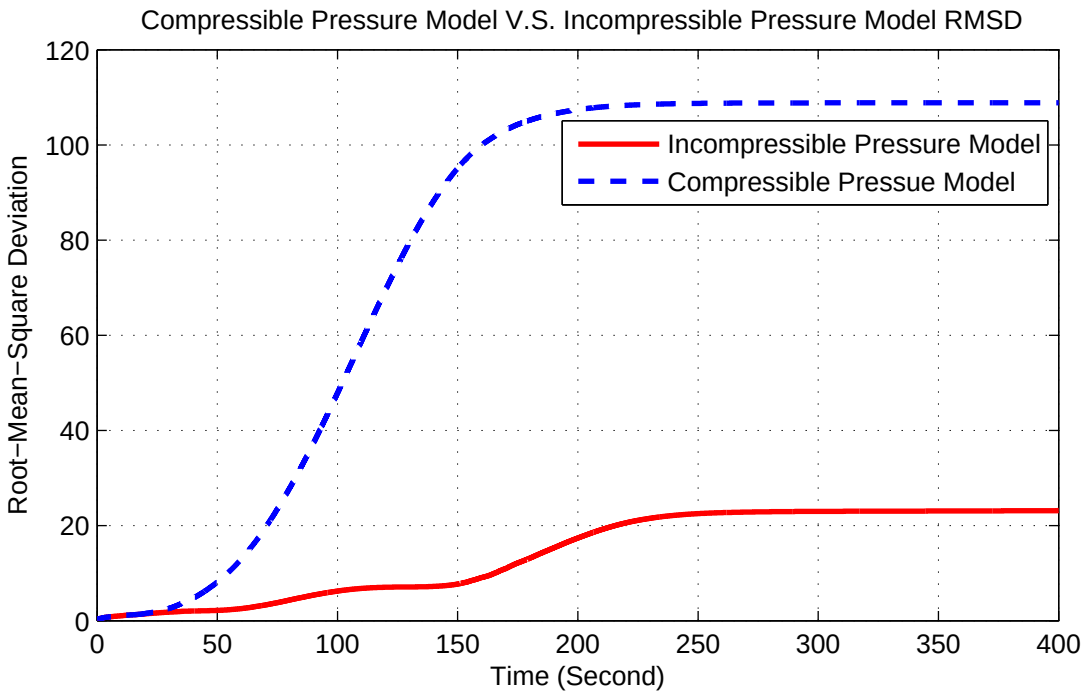

Figure 2.6: Compressible Model VS. Incompressible Model Root-Mean-Square Deviation

CHAPTER III

CONTROL STRUCTURE AND TUNING

In this chapter, two general purpose controllers are introduced, including PID and ADRC, as the candidates for the air pressure regulation system introduced in the last chapter. The chapter is organized as follows. PID control law is briefly reviewed in Section 3.1. The history of ADRC and the structure of LADRC are discussed in Section 3.2. The PID control tuning based on the linearized model is presented in Section 3.3. Finally, the tuning process of ADRC is described in Section 3.4.

3.1 PID Controller

The basic idea behind the PID control strategy is dated back to the 1780s in Watt's flyball governor design for the speed regulation in steam engine. The flyball governor is essentially a proportional control mechanism in today's term. In 1868, the famous physicist James Clerk Maxwell analyzed such control system in the famous paper "On governors" [59], which is widely considered a classic founding paper in feedback control theory. It was the first time differential equations were used to analyze control systems. The proportional control was later enhanced by adding

the integral and derivative terms. In 1922, Nicholas Minorsky first formalized the three-term PID controller [60]. Since then, PID controller as a simple and efficient control law has dominated industry controls to this day.

The algorithm of PID controller is given by the formula:

$$u(t) = K_p e(t) + K_i \int_0^t e(T)dT + K_d \frac{d}{dt} e(t) \tag{3.1}$$

where u is the control signal and e is the tracking error between reference value (set point) and output. The control signal is the sum of three terms, where the proportional term P represents the present, the integral term I represents the past, and the derivative term D represents the future trend. The controller parameters are proportional gain K_p, integral gain K_i and derivative gain K_d. This controller is designed to drive the error to zero. In particular, the integral term was added when people found that the proportional control alone often leads to significant steady state error and adding the integral control will help solve this problem. But this is done at the cost of reduced stability margin, since the integral control brings additional phase lag into the system. The derivative control term helps to address the phase lag but itself often runs into noise issues, since all output measurements are subject to noise contamination.

It is therefore clear that the PID control law, although simple and popular, is always a compromise. Every term must be carefully calibrated since too little and too much both bring ill effects to the system. The fundamental limitation of PID comes from its core design principle: error-driven feedback control. In such control systems, the control action is always lagging behind because it can only react to tracking error after the error has appeared, not to prevent error from taking place beforehand. It is for this reason we turn to ADRC as a possible alternative to PID.

3.2 ADRC

While PID has dominated industrial control for the last century, we have seen rapid developments in control theory first in classical control theory of the 1940s and then the modern control theory since the late 1950s. Classical control theory didn't replace PID but it helped people understand better the nature of feedback control systems, particularly their stability characteristics. The transfer function and the frequency response method have become very useful tools of analysis for practitioners; terms like bandwidth and stability margin have become standard vocabulary for engineers. But the corresponding design method known as loop-shaping, although potentially much more powerful, proves to be too cumbersome to be used as a general purpose design tool for daily use.

Modern control theory was born in the late 1950s and it has been developed rapidly since then, in which the analysis and design of control system is mainly through the description of the state space model in time domain. Modern control theory can handle control problems much more widely, including linear and nonlinear systems, time–invariant and time–varying systems, single variable and multi–variable systems, etc. The main motivation for modern control theory is to obtain the optimality in the performance of control systems, and optimality can only be obtained rigorously based on the detailed and accurate the mathematic model of the plant. Because of this reason, building the mathematic model of the controlled object, analysing the model of the real system and designing a control law based on the model have become the standard way of solving a control problem. In doing so, modern control theory is obsessed with obtaining the model and controlling it, to the detriment of understanding and solving engineering problems, which are dominated by the uncertainties. Pushing this to the extreme could eventually leads to what is described by J. Han as the "model disaster". The solution, as Han suggested, is ADRC [37].

The basic structure of ADRC is shown in Figure 3.1 with the controller-rejector pair. The basic idea of simplify controller design and maintaining a consistent performance is not to let the con-

troller interface directly with the messy physical processes, full of nonlinearities and uncertainties. Instead, the controller's task of meeting the design specifications becomes a lot easier when it deals with only the enforced plant, which is the modified plant after the effects of the disturbances are removed by the rejector. Comparing to the original physical plant, the enforce plant tends to be much simpler and less uncertain. This is the key in overcoming the weakness of PID and in making control action much more proactive in addressing the cause of the tracking error, not simply reacting to it.

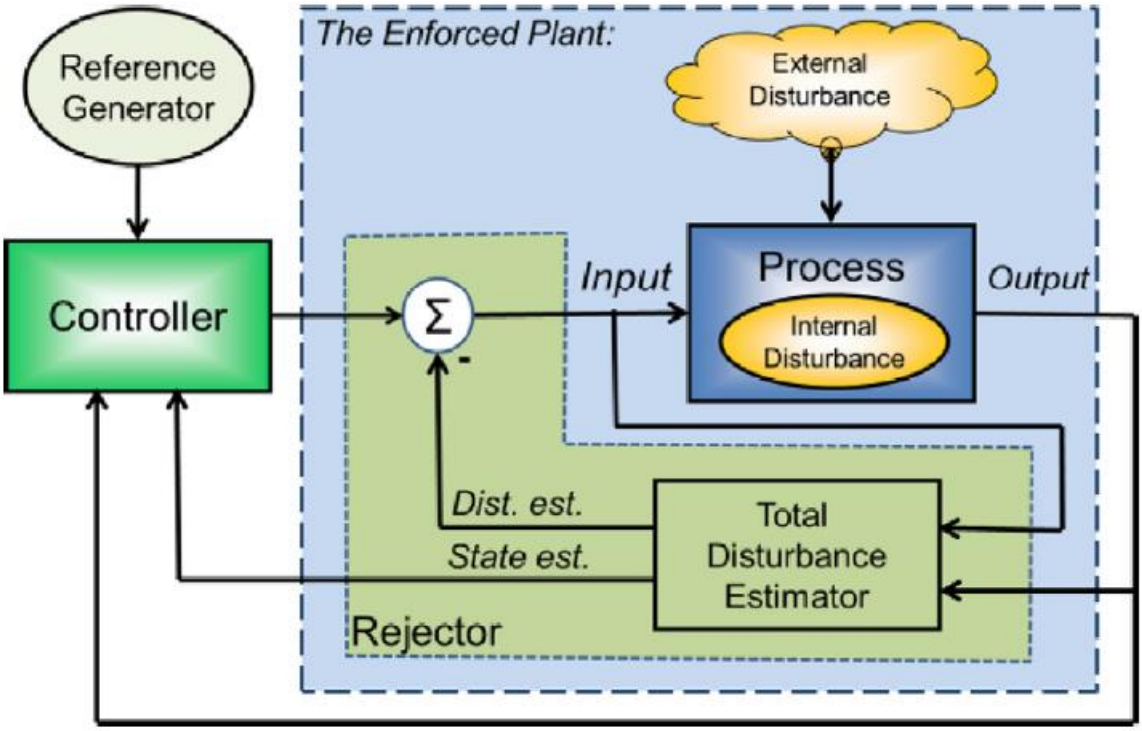

Figure 3.1: Disturbance Rejection Control Platform [28]

To illustrate the ADRC design in the context of the air pressure system described in the previous chapters, consider a general first–order plant:

$$\dot{y} = f(y,d,u,t) + b(u) \tag{3.2}$$

where y is the system output, d is the external disturbance, u is the control signal, and b is the constant coefficient. Here the enforced plant is considered as the ideal integrator and $f(y,d,u,t)$ represents the total disturbance in the plant, including both the internal and external disturbances. The mainly idea here is to estimate the total disturbance and cancel it using the control signal to form the enforced plant, which is a simple integral plant with a scaling factor of b. This makes the controller design a much easier task.

Assuming that the approximate value of b is given as $b_0 \approx b$, and denoting $f(y,d,u,t)$ simply as f. Eq. (3.2) can be rewritten as

$$\dot{y} = f + b_0 u \tag{3.3}$$

The critical task at this stage is to estimate total disturbance f and this can be done using the state observer approach from the modern control theory. In particular, if the total disturbance f can be treated as a state variable, known as the extended state, and the new state space model of the plant is observable, then a state observer can be design to estimate not only the original state variables but also the extended state. Such observers are known as the extended state observer (ESO) and it is derived as follows.

The plant in Eq. (3.3) is written in form of the state equations, let $x_1 = y, x_2 = f$. Assume f is differentiable, or $h = \dot{f}$ exists, the plant can be described in state space form as

$$\begin{cases} \dot{x_1} = \dot{y} = x_2 + b_0 u \\ \dot{x_2} = \dot{f} = h \end{cases} \tag{3.4}$$

where $y = x_1$

Rewritten Eq. (3.4) as

$$\begin{cases} \dot{x} = Ax + Bu + Eh \\ y = Cx \end{cases} \tag{3.5}$$

where

$$A = \begin{bmatrix} 0 & 1 \\ 0 & 0 \end{bmatrix}, B = \begin{bmatrix} b_0 \\ 0 \end{bmatrix}, E = \begin{bmatrix} 0 \\ 1 \end{bmatrix}, C = \begin{bmatrix} 1 & 0 \end{bmatrix}$$

Then the ESO can be constructed as:

$$\begin{cases} \dot{z} = Az + Bu + L(y - \hat{y}) \\ \hat{y} = Cz \end{cases} \tag{3.6}$$

where the observer gain vector L is chosen that all the observer poles are at $-\omega_o$, the negative bandwidth of the observer which use the bandwidth–parameterization and optimization method to make the ESO have only one parameter $-\omega_o$ to tune [38].

$$L = \begin{bmatrix} 2\omega_o & \omega_o^2 \end{bmatrix}^T$$

After tuning observer bandwidth ω_o properly, y and f can be tracked closely by z_1 and z_2. The control law is

$$u = \frac{-z_2 + u_0}{b_0} \tag{3.7}$$

Apply the control law Eq. (3.7) to Eq. (3.3) and ignore the estimation error, the original plant can be reduced to a single–integral system

$$\dot{y} = u_0 \tag{3.8}$$

which is easily controlled by a proportional controller

$$u_0 = k_p(r - z_1)$$

where r is the set point, the controller gain $k_p = \omega_c$, ω_c is the controller bandwidth that is placing the closed–loop poles at $-\omega_c$.

From the above derivations one can see: simple structure, wide applications, independence of the process model, good control performance, strong robustness, and easy to tune are all the advantages of ADRC.

3.3 PID Tuning

For the purpose PID tuning, the model of the plant is first linearize. Substituting the parameters of the actual plant into the Eq. (2.27), the differential equation of the plant is given as:

$$\dot{x} = 1.85\sqrt{735670.6 - x}(u - 1) \tag{3.9}$$

where x is the pressure output. Since most of the control law is developed on a linear system. The Jacobian linearization is applied to the plant model about a specific operating point (equilibrium point). Suppose $(\bar{x}, \bar{u})$ is an equilibrium point and the input,

$$\begin{cases} \delta x(t) = x(t) - \bar{x} \\ \delta u(t) = u(t) - \bar{u} \\ \dot{\delta} x(t) = f(\bar{x} + \delta x(t), \bar{u} + \delta u(t)) \end{cases} \tag{3.10}$$

Then, the right hand side of Eq. (3.10) can be approximated by a Taylor series expansion about the equilibrium point, neglect all higher (higher than 1st) order terms and let $(\bar{x} + \bar{u}) = 0$, we have,

$$\dot{\delta}(t) \approx \frac{\partial f}{\partial x}|_{u=\bar{u}}^{x=\bar{x}} \delta x(t) + \frac{\partial f}{\partial u}|_{u=\bar{u}}^{x=\bar{x}} \delta u(t) \tag{3.11}$$

From the Eq. (3.9), it is obviously that there are infinites equilibrium points, for example: $x = 735670.6$, u as arbitrary value or $u = 1$, x as arbitrary value. The critical operating point is $\bar{x} = 515040$,$\bar{u} = 1$, because the set point is 515040 Pa. Thus, Eq. (3.9) can be approximated by a Taylor series approximation around the equilibrium point $(\bar{x} = 515040, \bar{u} = 1)$, the transfer function is approximately equal to:

$$\frac{y(s)}{u(s)} = \frac{752.55}{s} \tag{3.12}$$

This linearized model is used for the PID tuning based on the Ziegler–Nichols step response tuning method in MATLAB SISOTOOL, as shown in Fig.3.2, which produced the PI controller gains as $K_p = 0.00186$, $K_i = 0.00133$. In Fig.3.3, the open loop Root locus and bode plot of the automated tuning controller are displayed. However, this PI controller does not work since steady state error cannot be eliminated. Finally, based on the Ziegler–Nichols and trial–and–error tuning methods, a PI controller is retuned for the pressure control loop. The parameter of the PI controller is shown in Table. (3.1), and the simulation in MATLAB is shown in Fig.3.4.

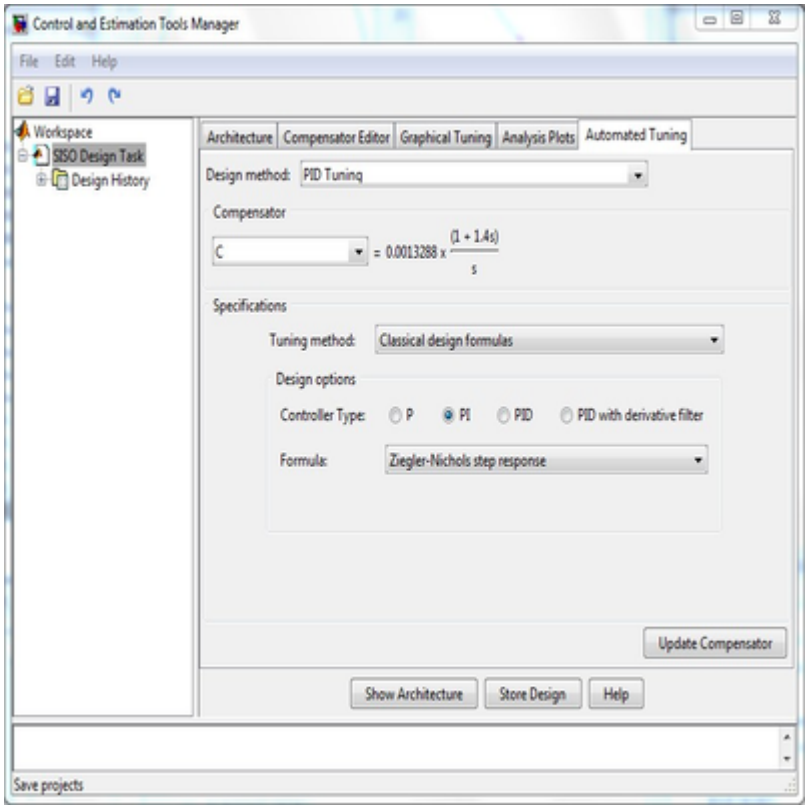

Figure 3.2: Automated Tuning in MATLAB SISOTOOL

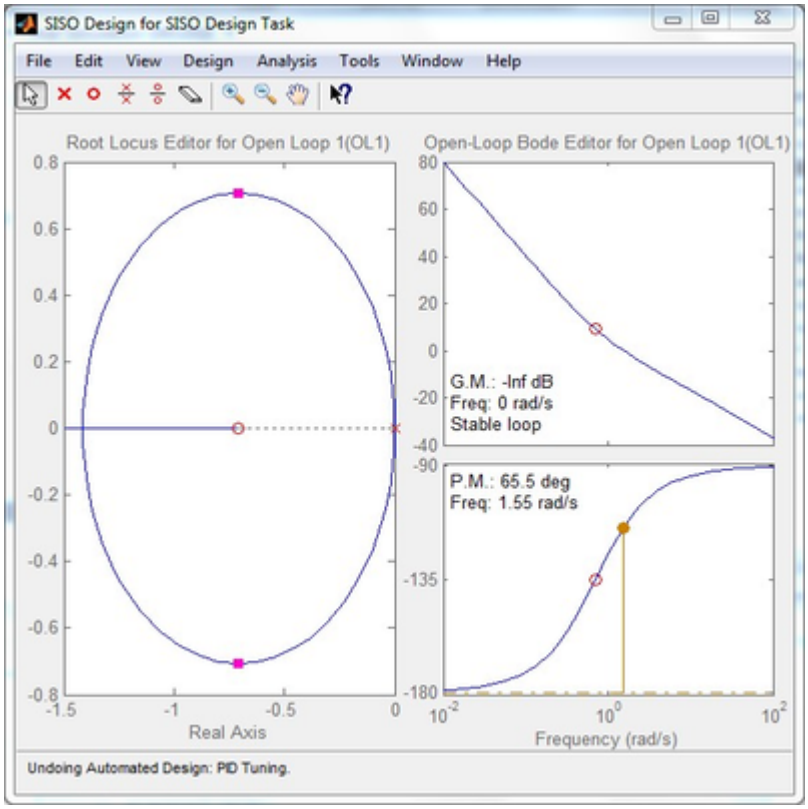

Figure 3.3: Open loop Root Locus and Bode Plot

Table 3.1: The Parameters of PI Controller

Parameters	**Values**
K_p	6
K_i	$4.12e-4$

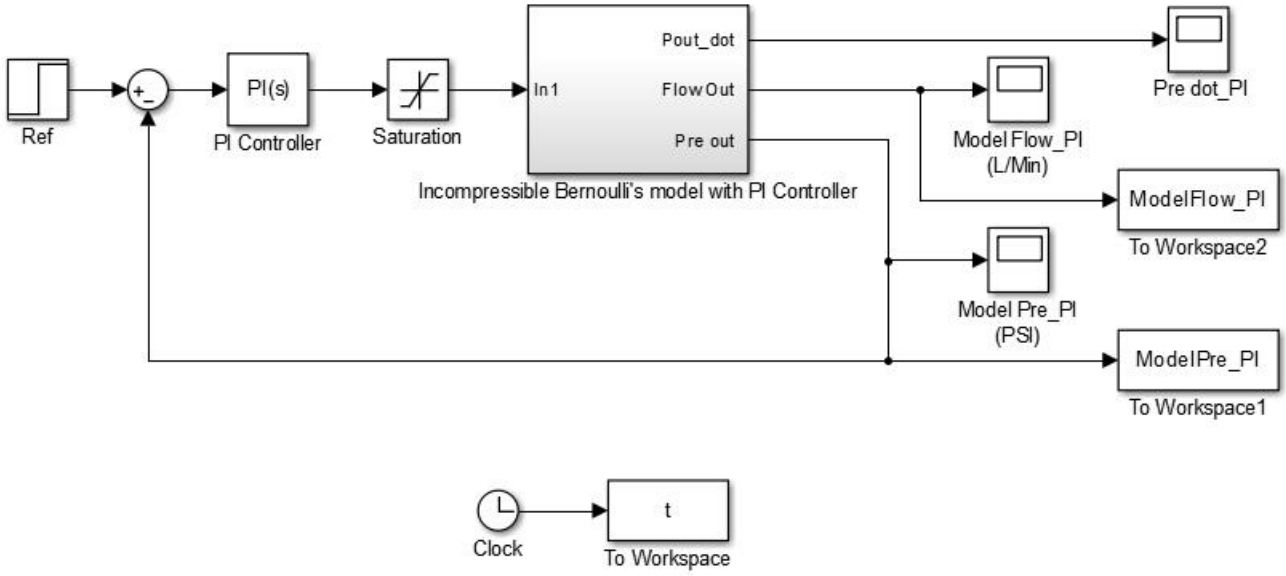

Figure 3.4: PI Closed loop MATLAB Simulation

3.4 ADRC Tuning

The original nonlinear ADRC has many parameters that need tuning. The LADRC is simplified with only three parameters to be determined: ω_c,ω_o,and b_o. Each of them has its own physical meaning: ω_c is the control bandwidth, ω_o is the observer bandwidth and the b_0 is the critical gain parameter and is the only information needed from the plant. Fig.3.5 is the MATLAB simulation structure of a 1st order system controlled by ADRC. It consists of three parts: controller, observer and plant. The controller part can be treated as P or PD controller, which depends on the order of the plant. In this project, the plant is a 1st order system, thus P controller is used. The observer part is made up of the observer gains and the ESO equations.

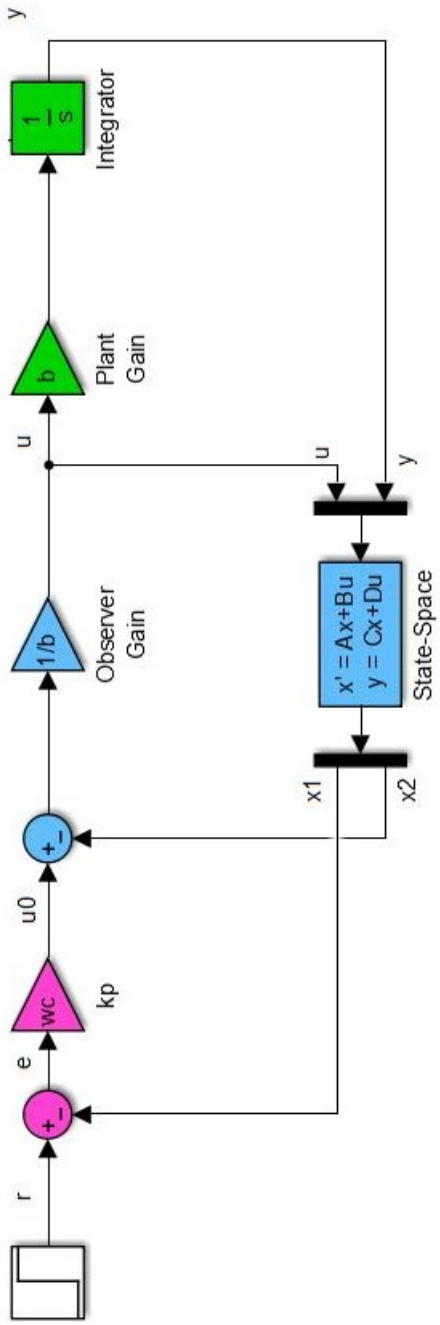

Figure 3.5: Simulation of a 1st Order System Controlled by LADRC

The first tunable parameter is ω_c. As we known, the higher bandwidth corresponds to better tracking performance. At the same time, the realizable bandwidth is limited by the existing

sensor noise and dynamic uncertainties. In this project, let the ω_c equal to the K_p to make a fair comparison for PI and ADRC.

The observer bandwidth corresponds to the frequency range where the total disturbance is estimated and canceled. For disturbance rejection, the larger ω_o is the better, subject to the same noise limitations mention above. Generally in state feedback control literature, it is suggested that the observer bandwidth should be 3 to 5 times larger than the control bandwidth. However, in this particular air pressure control system, $\omega_o = \omega_c$ is able to meet the requirements.

The critical parameter b_0 can be treated as given or as a tunable parameter. Usually the control engineers have some knowledge of the plant, from which an approximate value of b_0 can be obtained. For the complex system with a time varying b_0, it is not simple to obtain or tune the value of b_0. For this kind of system, b_0 can be implemented as a function of the output pressure and put into the ESO. However, this method requires familiarity with the structure of ESO. Thus, a sample method to determine the critical gain b_0 is proposed in this study based on the linearized model.

From the linearized plant model Eq. (3.9), it is clear that the critical gain parameter is

$$1.85\sqrt{735670.6 - x} \tag{3.13}$$

where the x is the output pressure. The b_0 is a function of the output pressure, which means that it is a time varying parameter. In addition, the Eq. (3.13) shows that the b_0 is a nonlinear function of the pressure. In order to obtain a simplified b_0, this function needs to be linearized. From the Section 3.1, it is shown that there are many equilibrium points in this system, the selection of equilibrium point is critical to determine the b_0. From the experiments, the equilibrium points close to the operation point can be used to obtain b_0. According to the Eq. (3.12), 752.55 is the value of b_0. Furthermore, because of the unit of the model is in international system of units (SI), but the unit of the set point is psig, the actual b_0 is 0.1 after the unit conversion from pascal to psig. Table. (3.2) shows all the ADRC parameters.

Table 3.2: The Parameters of ADRC Controller

Parameters	**Values**
ω_c	6
ω_o	6
b_0	0.1

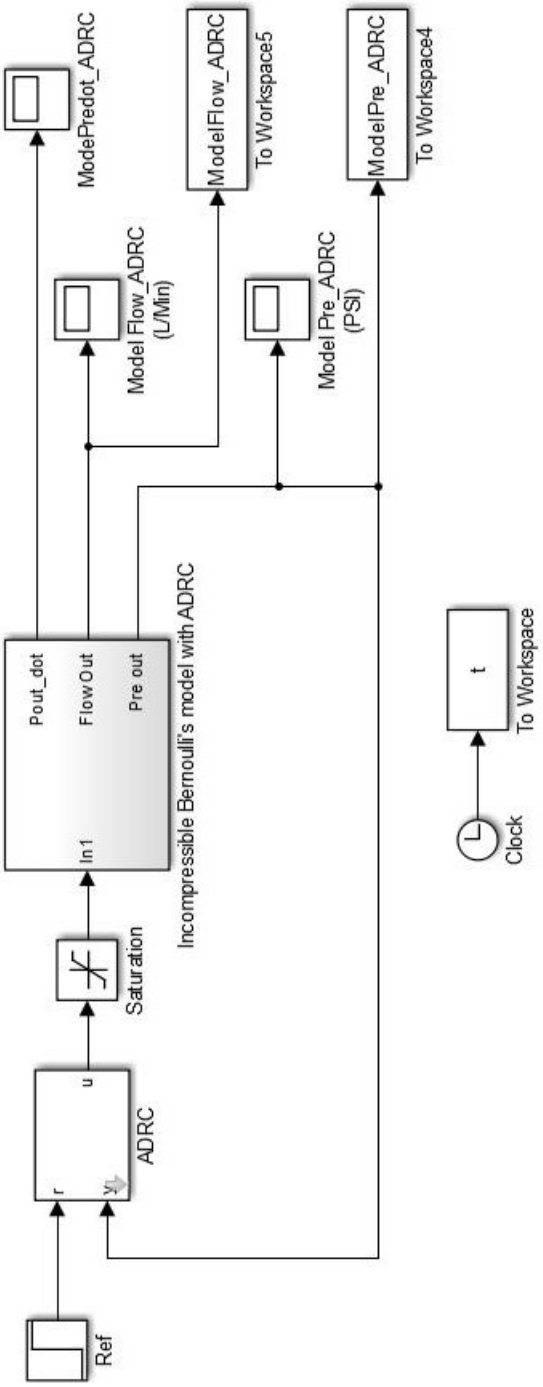

Figure 3.6: ADRC MATLAB Simulation

CHAPTER IV

SIMULATION STUDY

The properties and tuning of the general purpose PI and ADRC control algorithms described in Chapter III are studies in this chapter via simulation based on the mathematic models of the air pressure system. The simulation results are evaluated in terms of the tracking ability and the internal as well as external disturbances rejection capability. In particular, the tracking performance is tested using a multiple–step signal which is designed for both the simulation and experimental studies. By modifying the size of flow valve and the temperature in the tank, the internal disturbance is introduced to evaluate the disturbance rejection ability. In addition, load disturbance rejection and sensitivity to sensor noise are also considered.

4.1 Reference Tracking

To test the tracking performance of the PI and the ADRC controllers, a 60 psi step function with t=10 sec stepping time and the initial value of 3 psi is introduced as the set point for the output to follow. The tracking responses of the two control strategies are illustrated in Fig.4.1. Both controllers are tuned well and there is no significant difference the two except that the ADRC

response is a little faster than PI. The corresponding flow rates and the control signals are shown in Fig.4.2. Note that the flow rate, $1.28L/Min$, is consistent with the limitation of the real system. The control signal between 1 to 5 volts is shown in Fig.4.2, which reflects the constraint of the flow valve. The simulation results demonstrate both the proposed PI and ADRC controllers are able to satisfy the control requirements with the same control bandwidth. The results of the flow rate and the control signal are reasonable. But through the zoomed figure in Fig.4.1, the ADRC can be seen to have a shorter transient time than PI.

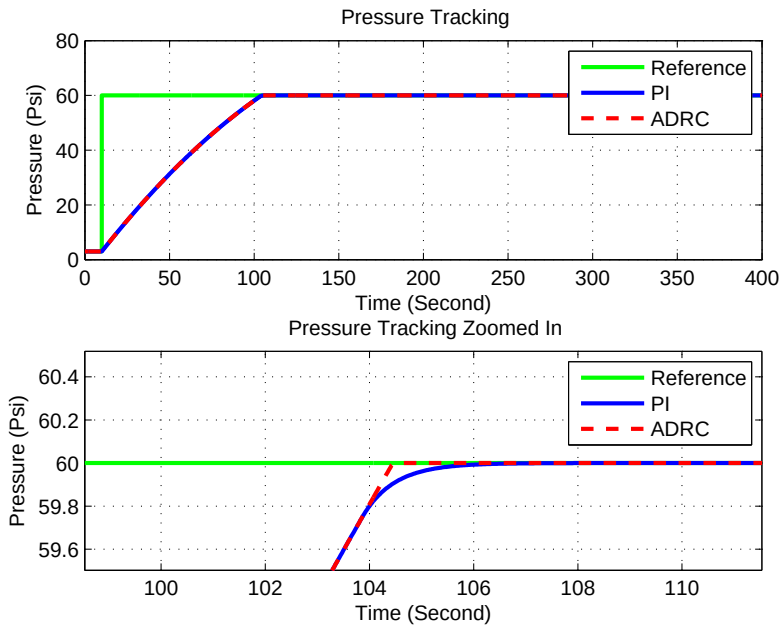

Figure 4.1: Pressure Tracking Response

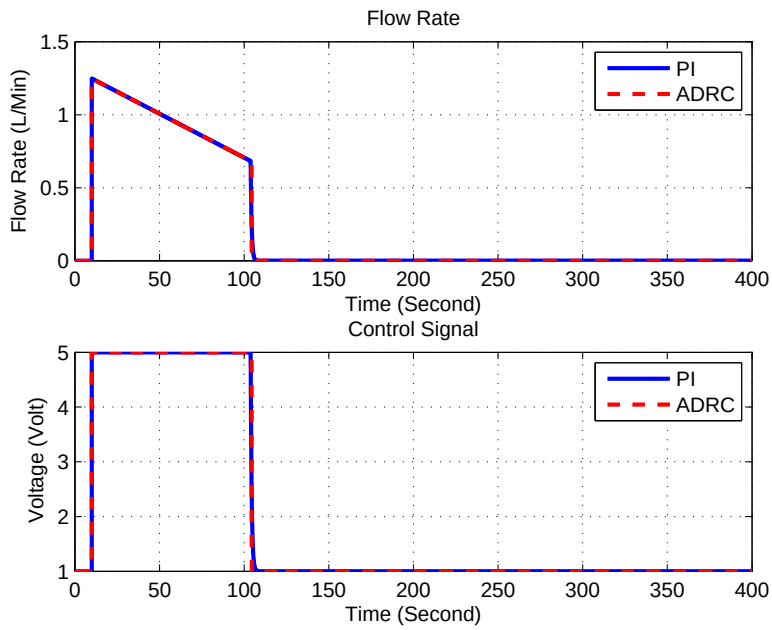

Figure 4.2: Flow Rate Response and Control Signals

For the case of variable reference tracking, the selected multiple-step signal is based on the physical characteristics of the real system. In the real system, the pressure can only be reduced by using the release valve, not the flow valve. Therefore, we only test the air pressure tracking with a variable step-up commands, to test the operating range of the pressure control system.

Fig.4.3 and Fig.4.4 show the tracking results together with the input trace from the mathematic model. The set point is a multiple-step signal with an initial value starting at 3 psi for the first 10 seconds and then jumps to the value of 35 psi and stay there until t = 150 sec. The second step has an initial value of 35 psi and the final value of 50 psi at t = 150 sec and stay there until t = 300 sec. The last step jumps to 75 psi at t = 300 sec and stays there until the end of the simulation at t = 400 sec.

From the tracking results, both controllers meet the requirement needs while limit the control signal to the range of 1 to 5V, without overshoot and ± 1 percent steady state error. However, the

result of PI controller has a slower transient response and 0.05 psi steady state error, this is shown in Fig.4.3. Therefore, it is concluded that ADRC is able to obtain a fast transient response and zero steady state error.

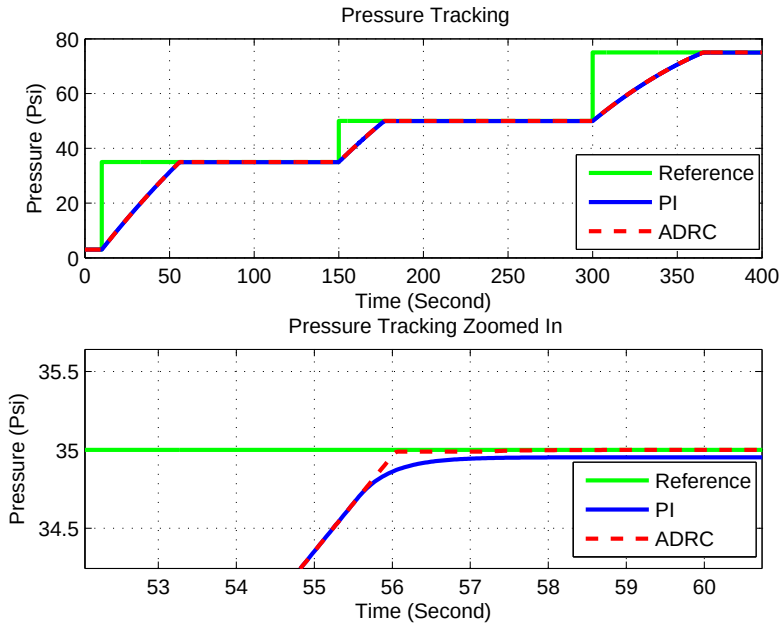

Figure 4.3: Multiple Steps Reference Tracking Response

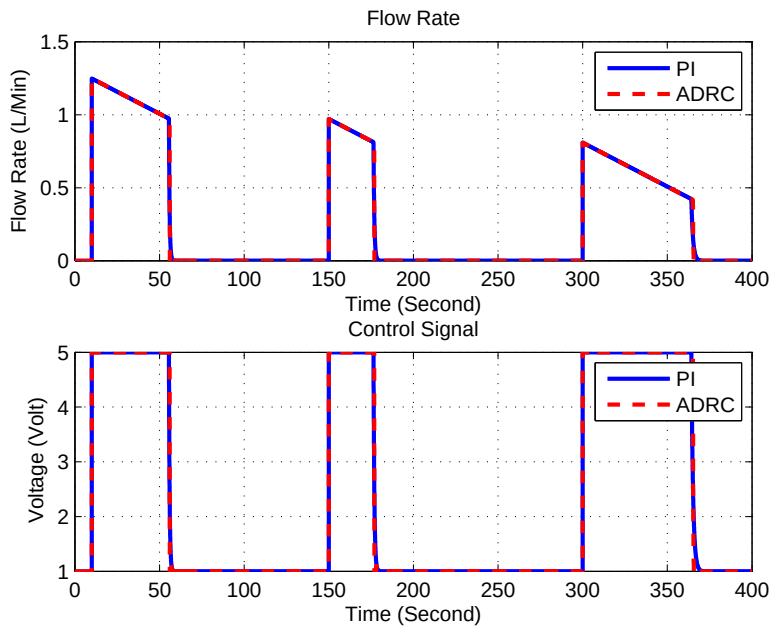

Figure 4.4: Multiple Steps Reference Flow Rate Response and Control Signals

4.2 Internal Disturbance Rejection

To study internal disturbance rejection, the flow valve size and room temperature are changed in the mathematic model to simulate the condition of adding internal disturbance to the plant. Such study is meaningful because replacing a component in the air pressure system is a common practice in industry during maintenance. In addition, replacing the existing valve with a larger one can increase the flow rate and decrease the transient response time. The question is how well the control system performance can be sustained with such variations in the components.

Fig.4.5 shows the results of increasing 4 times the area of the cross-section of the flow valve. Note that the pressure settling time is only 1/4 of the original settling time. Also, by raising the flow valve 4 times, the flow rate is increased 4 times as well. Thus, the maximum flow rate is reached at 5 L/Min shows in Fig.4.6. More importantly, based on the simulation results given in

Fig.4.5 and Fig.4.6, it is clearly seen that by increasing the valve size to 4 times larger than the original size, the control performance under PI and and ADRC is quite different. With ADRC, the change of the plant dynamics is actively rejected and the more robust performance is obtained, compared to PI.

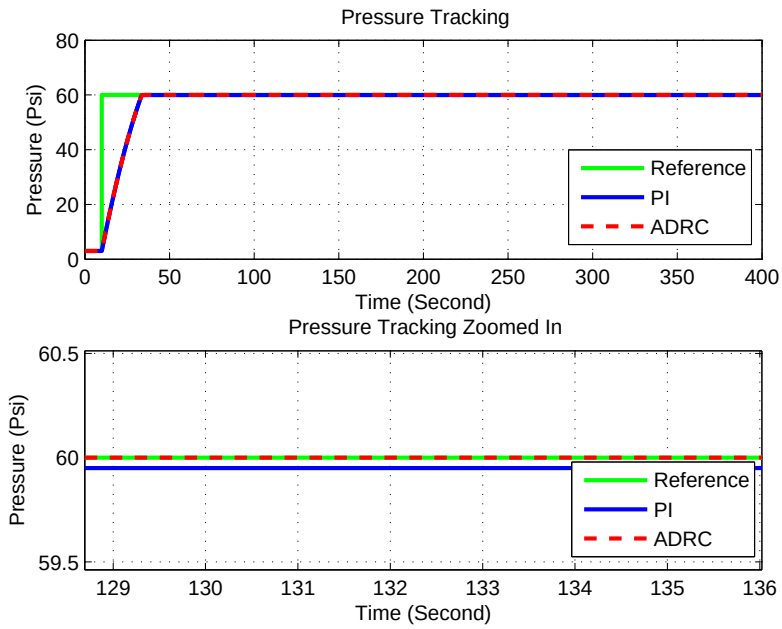

Figure 4.5: Tracking Response with Increased Valve Area (by 4 times)

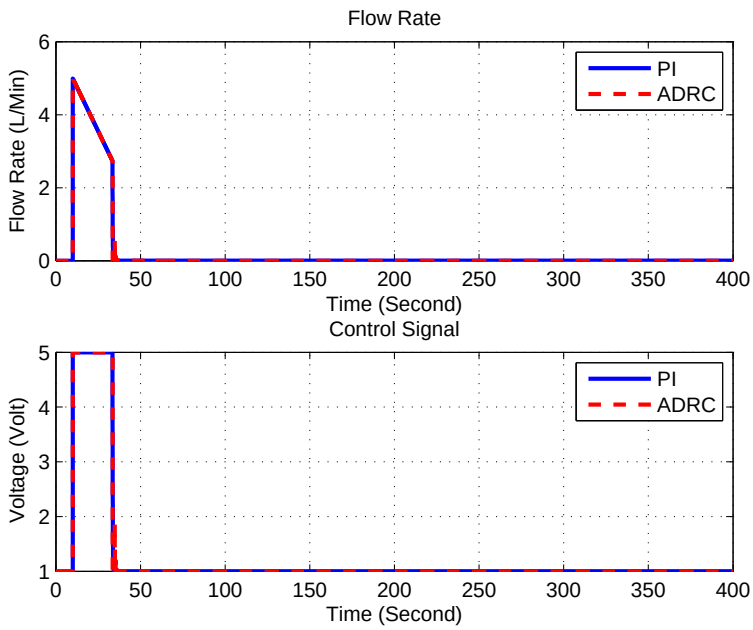

Figure 4.6: Flow Rate and Control Signal with Increased Valve Area (by 4 times)

Temperature variation is another important factor in process control. With air being compressed in the tank, the temperature within the tank is raised. Fig.4.7 shows that the air temperature in the tank has increased from 20 celsius to 40 celsius. From the simulation results it can be seen that the increase in temperature actually improves the transient response of the ADRC controller but degrades the transient response of PI, in addition to causing the steady state error as well. Thus, we conclude that ADRC has better performance than PI in term of temperature variation.

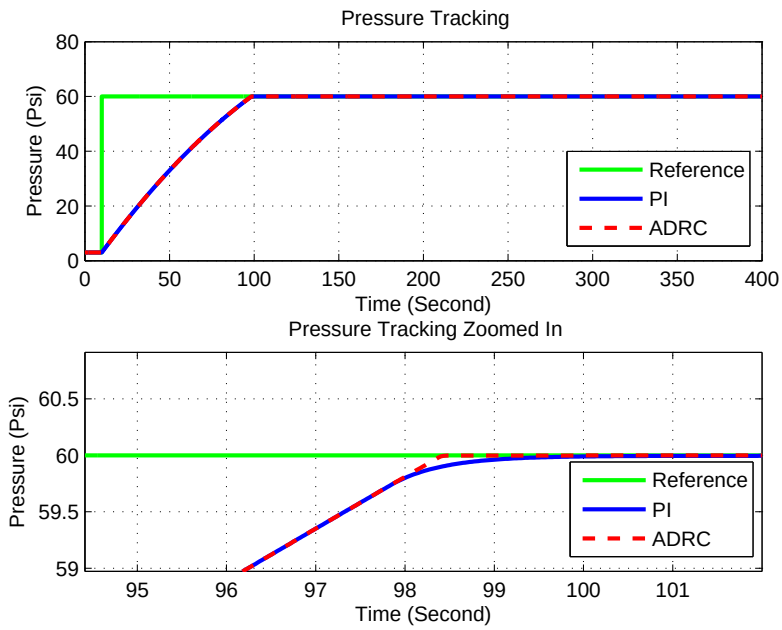

Figure 4.7: Tracking Response with Increasing Tank Temperature to 40 Celsius

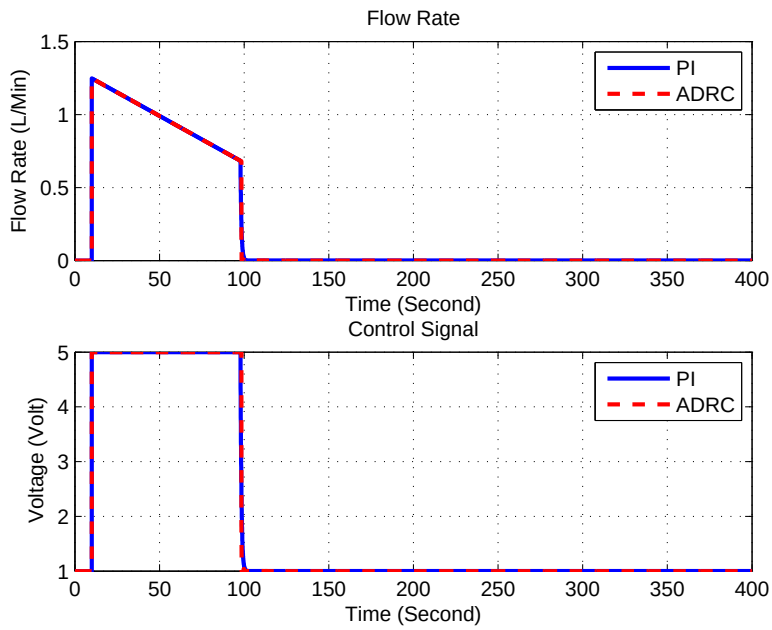

Figure 4.8: Flow Rate and Control Signal with Increasing Tank Temperature to 40 Celsius

4.3 External Disturbance Rejection and Noise Sensitivity

External disturbance rejection is probably the most important feature in practice, as well as the sensitivity to sensor noises. Step–type disturbance and band–limited white noise are added to control signal and the output feedback signal, respectively. Fig.4.9 and Fig.4.10 show how well both controllers perform in the presence of the external disturbance and sensor noises.

The physical meaning of the added disturbance is the air leakage in the tank. The timing for the disturbance to occur is set at 200 seconds, which is after the plant having reached the steady state. The effect of the disturbance alone is seen at the output. The simulation results, after adding disturbances of the values of 0.1 and 1.0 respectively, are shown in Fig.4.11 and Fig.4.13. It can be seen that as the external disturbances are introduced at 200 seconds individually in Fig.4.11 and Fig.4.13, respectively, the output tracking error is corrected immediately by the ADRC at 200 seconds and the disturbance effect is eliminated in less than 0.2 seconds. For the PI controller, however, the disturbance causes the steady state error that can not be removed. The larger the disturbance, the larger the steady state error. One can clearly see that after the disturbances are introduced at t = 200 sec, for the PI controller, the steady state error was caused and it became larger as the disturbance increases.

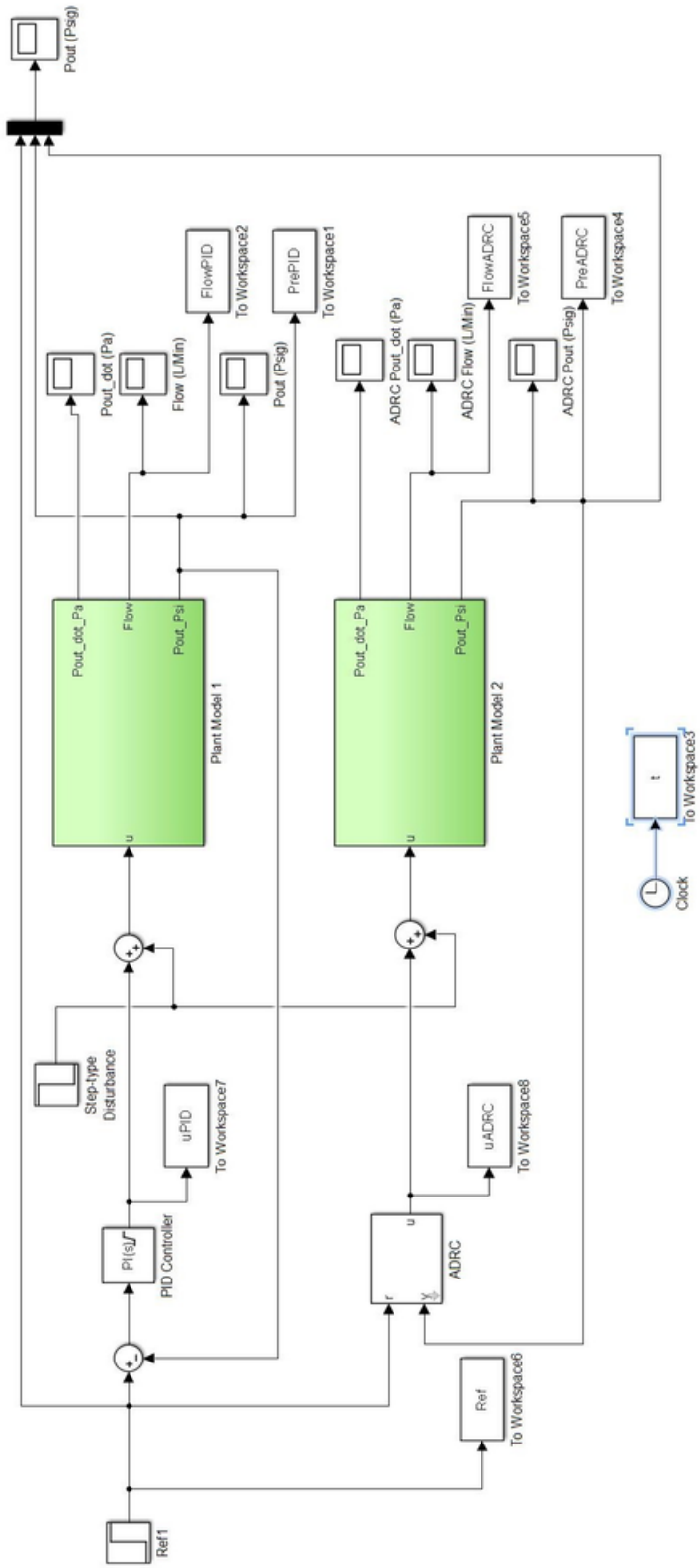

Figure 4.9: Matlab Simulink of Pressure and Flow System with Disturbance

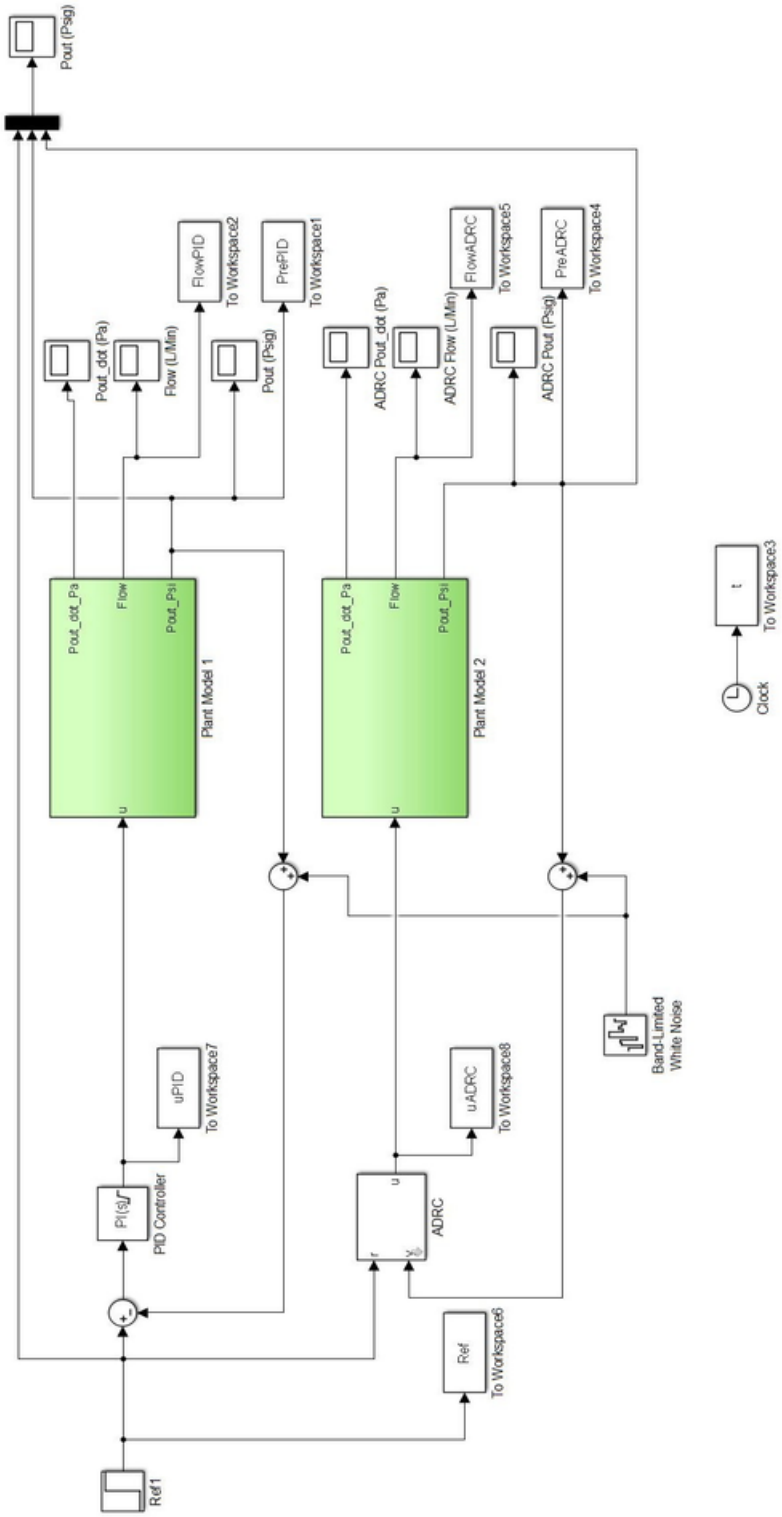

Figure 4.10: Matlab Simulink of Pressure and Flow System with White Noise

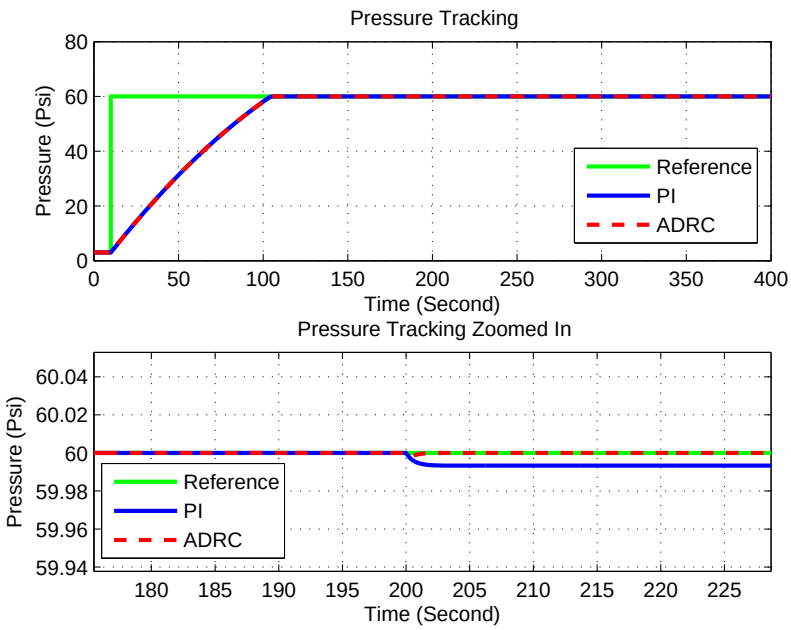

Figure 4.11: Tracking Response with Disturbance 0.1

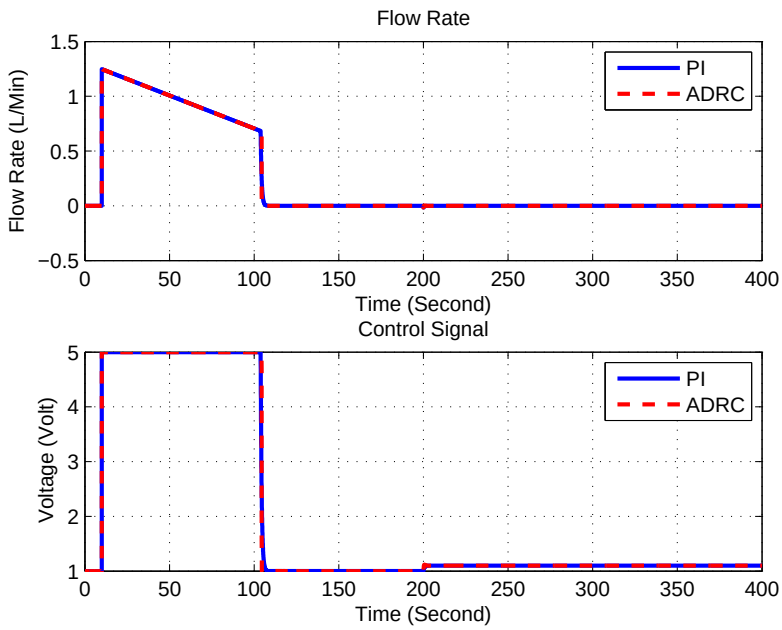

Figure 4.12: Flow Rate and Control Signal with Disturbance 0.1

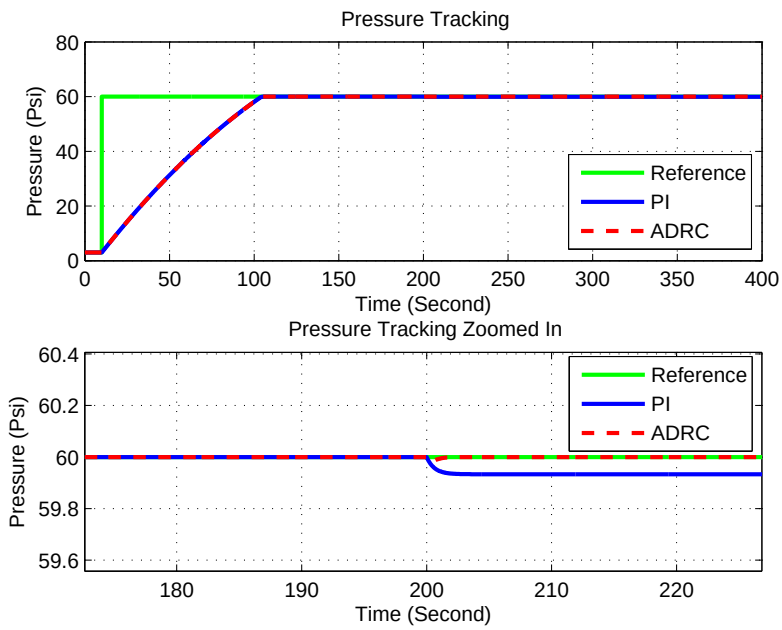

Figure 4.13: Tracking Response with Disturbance 1.0

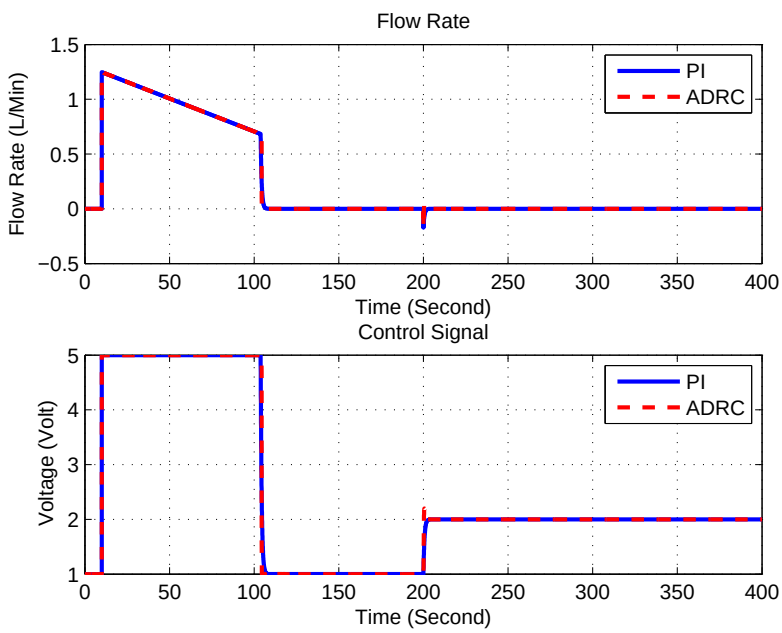

Figure 4.14: Flow Rate and Control Signal with Disturbance 1.0

Sensor noises are unavoidable in practice, typically in the range of 0.01 percent to 0.1 percent of the maximum output value, although some are even worse. The effect of such noises cause control signal to be very noisy which, in turn, can cause excessive wear and tear in the actuators. Fig.4.15 shows the sensor noise test results when white noise is introduced to both control system. From Fig.4.15 it can be seen that both PID and ADRC have the steady state error, because the control signal u is asymmetrical. This is because physically the upstream pressure of the valve is 92 psig, which is higher than the downstream pressure of 60 psi. Therefore, the valve can only keep or increase the pressure in the tank, but not decrease it. The noise also causes the tracking error and control signal to become noisy for both PI and ADRC controllers, as shown in Fig.4.16. The response of ADRC seems to meet the requirements better.

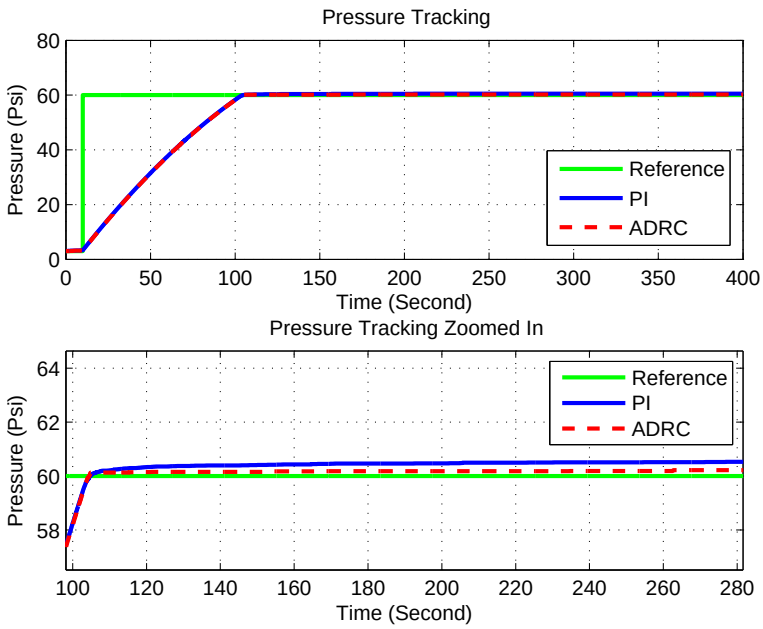

Figure 4.15: Tracking Response with 0.001 White Noise

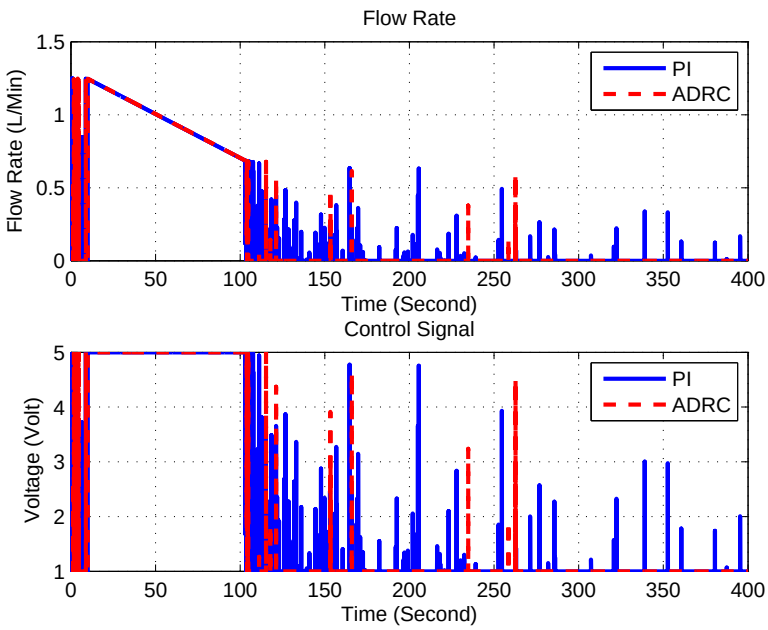

Figure 4.16: Flow Rate and Control Signal with 0.001 White Noise

CHAPTER V

EXPERIMENTAL STUDY

From the simulation results, it can be seen that ADRC is capable of realizing all the functions of PID; moreover, ADRC holds an absolute advantage in terms of disturbance rejection over PID. In this chapter, PID controller and ADRC controller are implemented in the experimental setup for the purpose of further validation. Both the reference tracking and disturbance rejection are tested. The energy consumption comparison is also demonstrated at the end of this chapter.

5.1 Reference Tracking

Because of the deviation of the mathematic model in describing the real system, both the PI and ADRC algorithms used in the simulation study are slightly modified to control the real system. All tuning parameters are shown in Table. (5.1). In order to make a fair comparison between the control bandwidths for both systems are kept at the same value of 6 r/s. All experiments of the real system are designed corresponding to the simulation studies. The tracking ability and the disturbance rejection ability are first tested and the experiment results are then explained.

PI	$K_p = 6$	$K_i = 0.01$	-
ADRC	$\omega_c = 6$	$b_0 = 0.6$	$\omega_o = 6$

Table 5.1: PI and ADRC Tuning Parameter for Real System

Similar to the simulation study, a 60 *psi* step is used as the reference to test the performance results of the proposed PI and ADRC controllers in the experiments. Fig.5.1 and Fig.5.3 show that the pressure tracking and flow rate tracking responses of both controllers are nearly the same. However, from the zoomed in Fig.5.2, it indicates that the PI controller has a 0.5 *psi* steady state; no steady state error for ADRC is found. In addition, Fig.5.3 demonstrates that the control signal of the PI controller has more oscillations than the ADRC controller. In short, the experiment results are consistent with the simulation results.

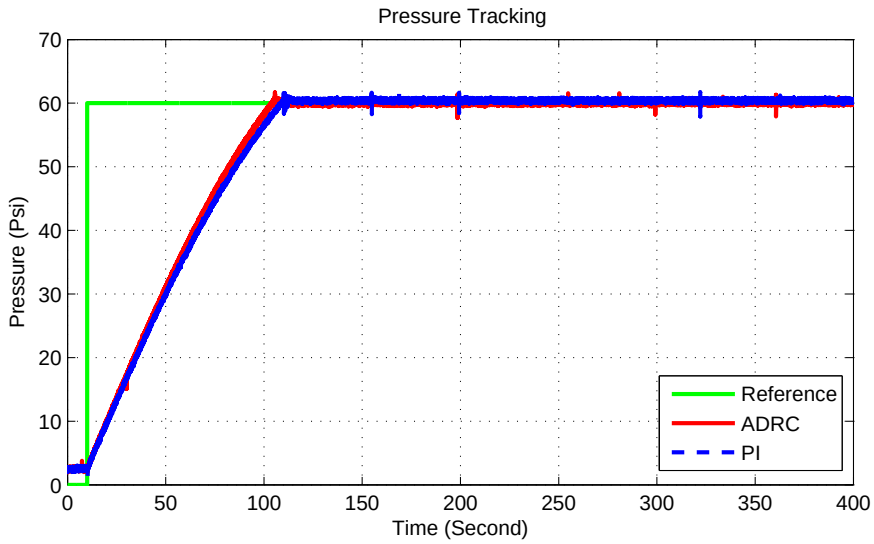

Figure 5.1: Real System Pressure Tracking

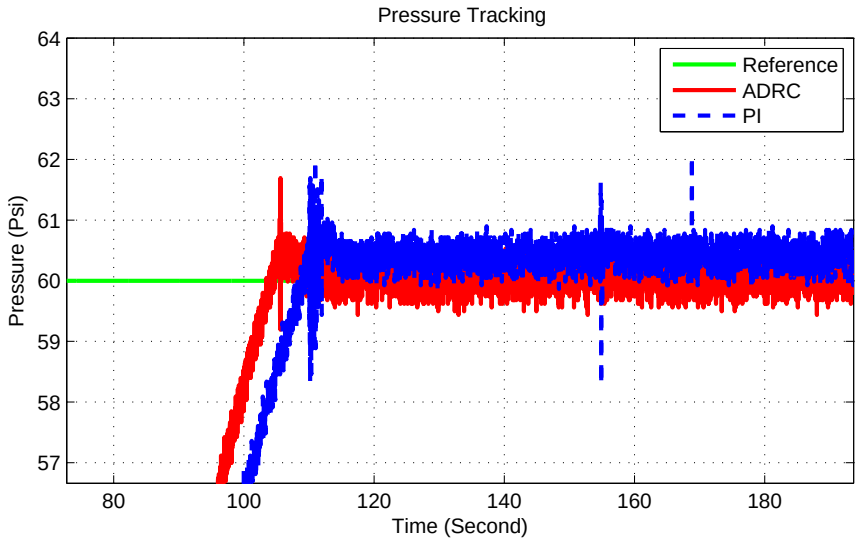

Figure 5.2: Zoomed in Real System Pressure Tracking

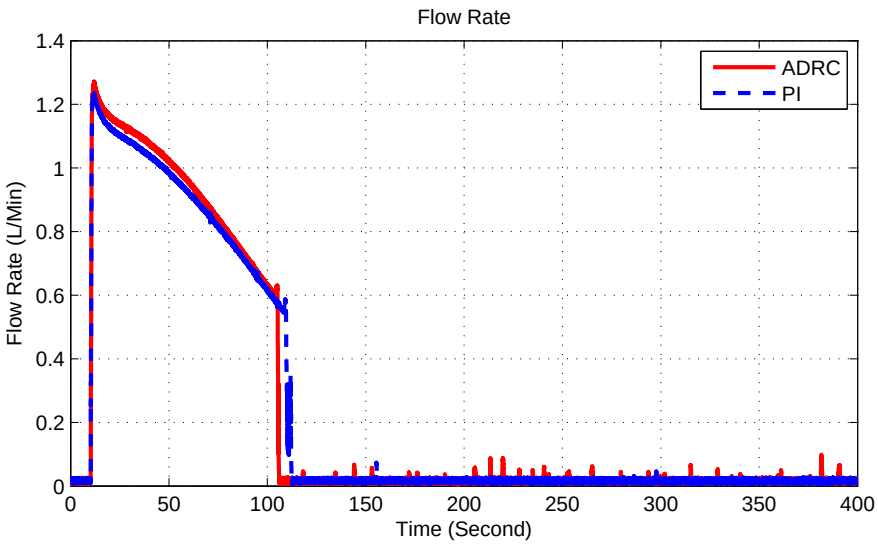

Figure 5.3: Real System Flow Rate Response

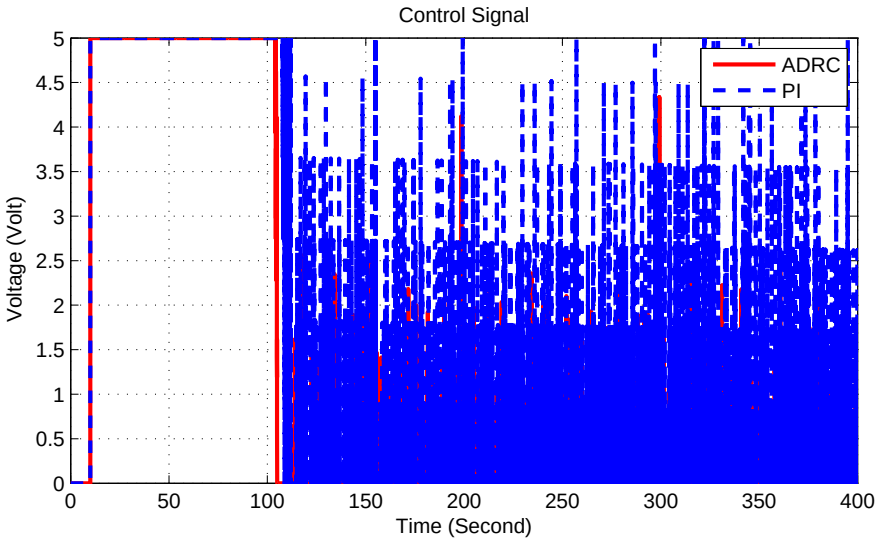

Figure 5.4: Real System Control Signal

The same multiple–step signal as the simulation reference tracking is used to test the tracking response for the real system. Fig.5.5 illustrates that there is ADRC is able to track the set point but PI is not during the first segment of the multi-step tracking. Nevertheless, on the second and third step commands, the both output responses are able to converge to the reference but with some steady state error in PI, as seen in Fig.5.6.. The flow rate tracking responses are reasonable in Fig.5.7, and yet the control signal of the PI is more oscillatory than the ADRC.

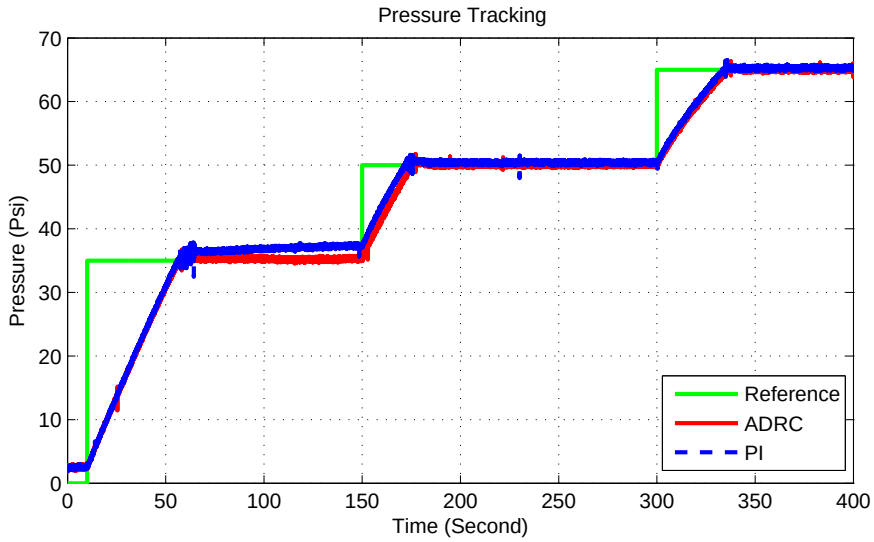

Figure 5.5: Pressure Tracking Response of Multiple Step Reference

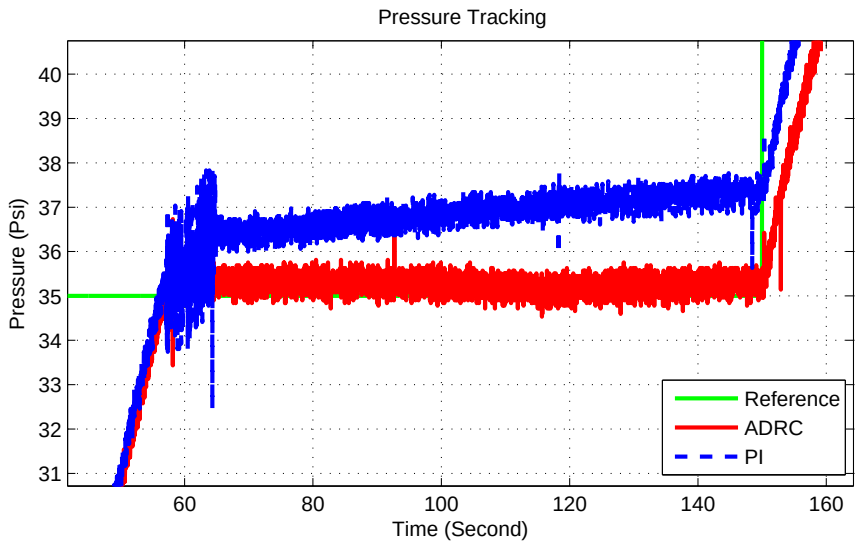

Figure 5.6: Zoomed in View of Pressure Tracking of Multiple Step Reference

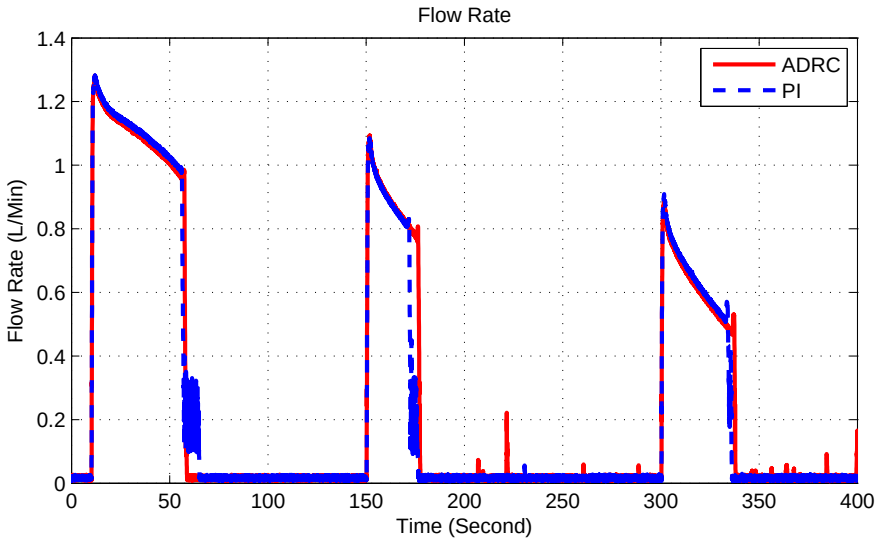

Figure 5.7: Flow Rate Tracking Response to Multiple Step Reference

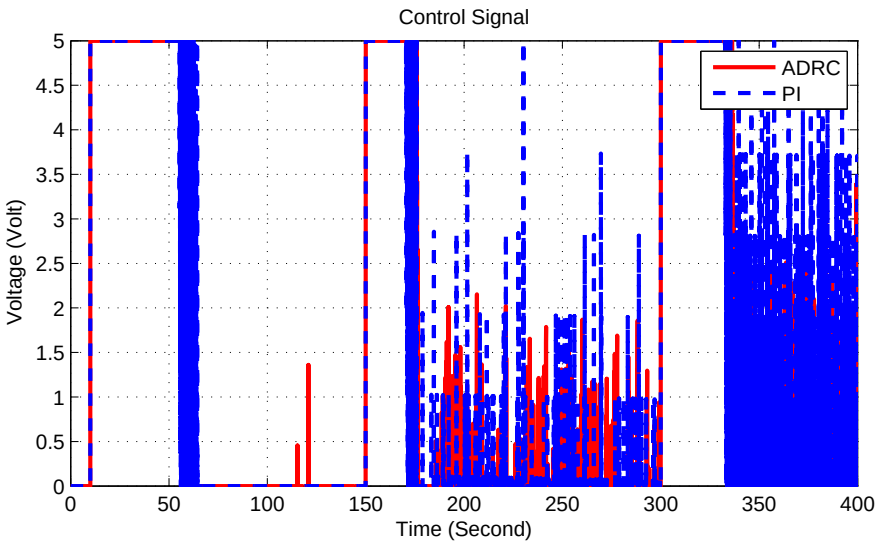

Figure 5.8: Control Signal for Multiple Step Reference

5.2 Disturbance Study

By opening the back pressure release valve at t = 200 *sec*, 1 *psi* leaking of the tank is introduced in the system after the response reached a steady state. The experimental response to the 1 *psi* leakage are shown in Fig.5.9. The zoomed in disturbance rejection period is shown in Fig.5.10, the PI and the ADRC are able to start correcting the output tracking error at t = 201 *sec*, and reject the disturbance to set point in 6 seconds. However, for the PI controller, a big oscillation happened at t = 204 *sec* and it continued until t = 206 *sec*; the steady state error is also appearing in the graph. The flow rate response is shown in Fig.5.11, at t = 201 *sec*, and it can be seen that the flow rate is increased to reject the leaking disturbance, and returns to the original value at t = 206 *sec* afterwards.

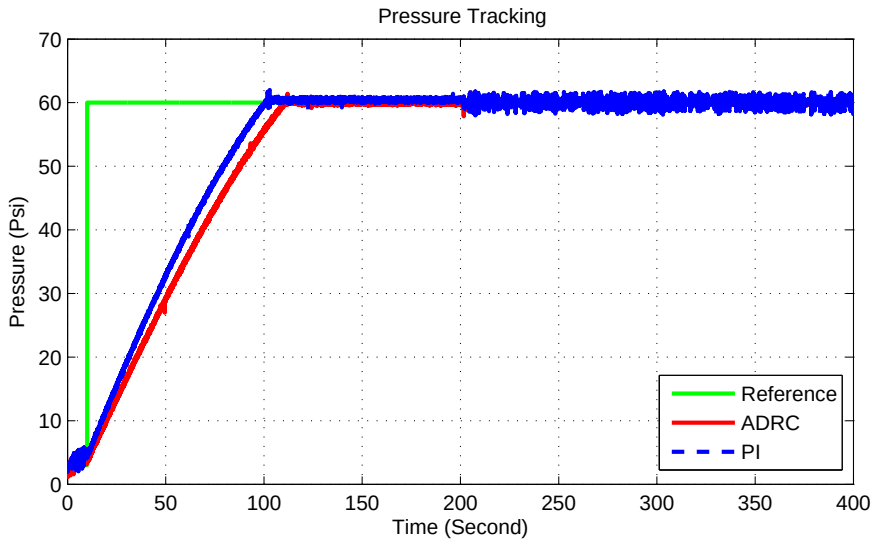

Figure 5.9: Real System Pressure Tracking with Disturbance

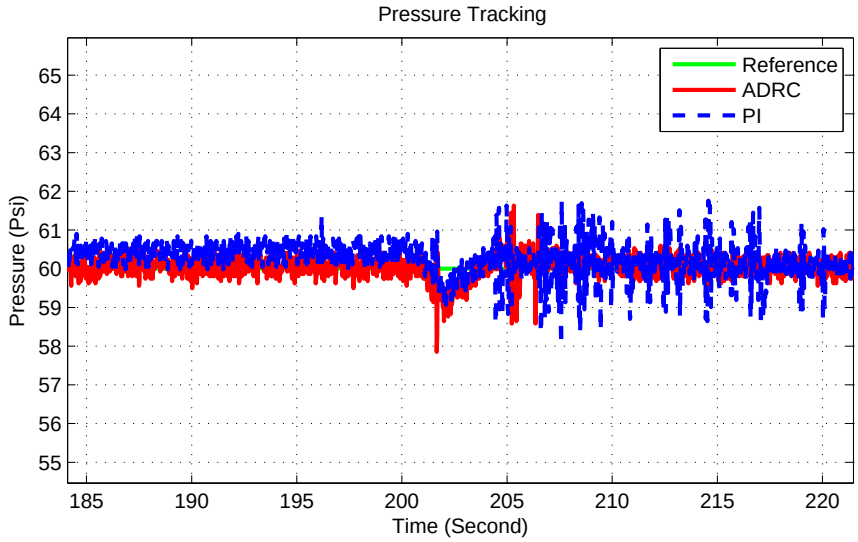

Figure 5.10: Zoomed in View of Real System Pressure Tracking with Disturbance

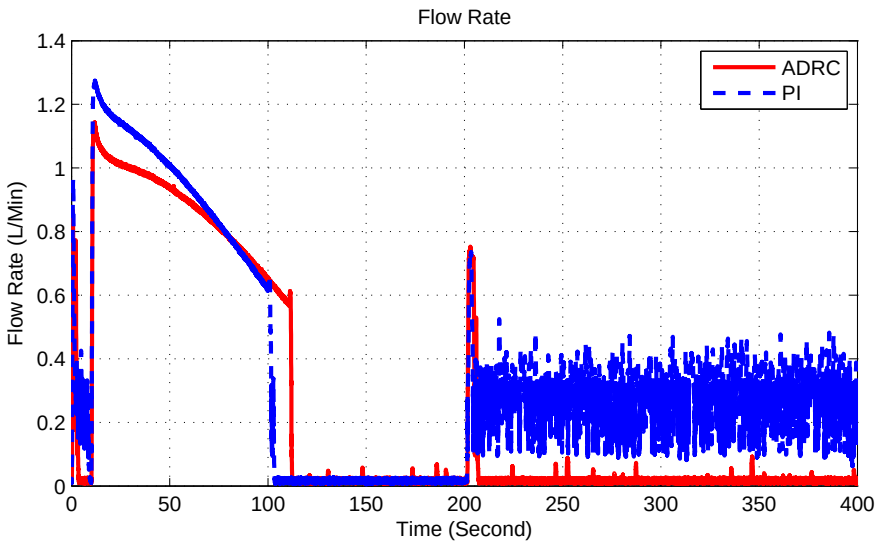

Figure 5.11: Real System Flow Rate with Disturbance

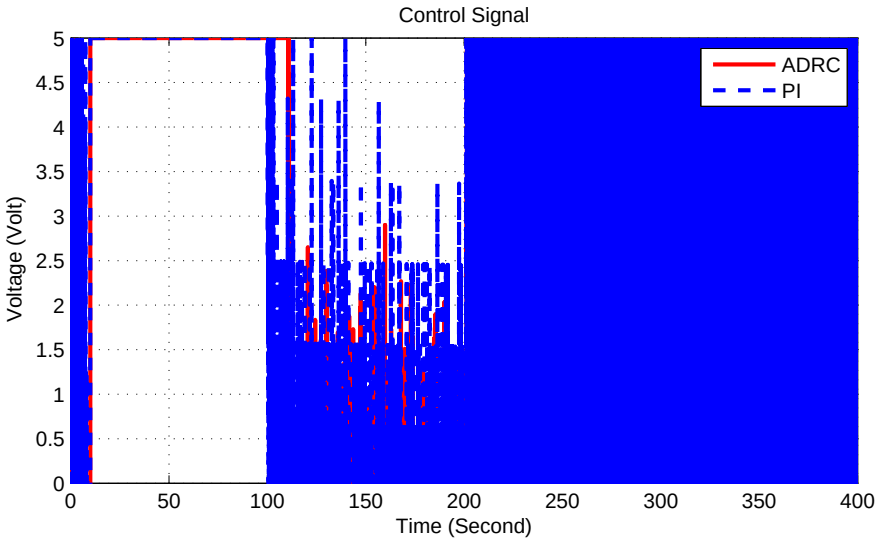

Figure 5.12: Real System Control Signal with Disturbance

5.3 Energy Consumption Study

Energy saving is one of the most important factors in industry and the control signal is a very critical indicator of energy consumption. Through integrating the square of the control signals, the energy consumption can be obtained. Fig.5.13 shows the energy consumption of the control signal of regular pressure tracking. It is clear that ADRC consumes less energy than PI at the similar performance level with perhaps a slightly faster transient response. The energy consumption of the multiple steps reference pressure tracking is demonstrated in Fig.5.14. Since the ADRC is more responsive and has better tracking than PI, it is reasonable to see that the PI control spends less energy. As shown in Fig.5.15, however, ADRC expends significant less energy than the PI control in disturbance rejection, because of the weakness of the disturbance rejection in PI, leading to oscillations in the control signal and energy waste. Overall, the ADRC presents higher energy efficiency.

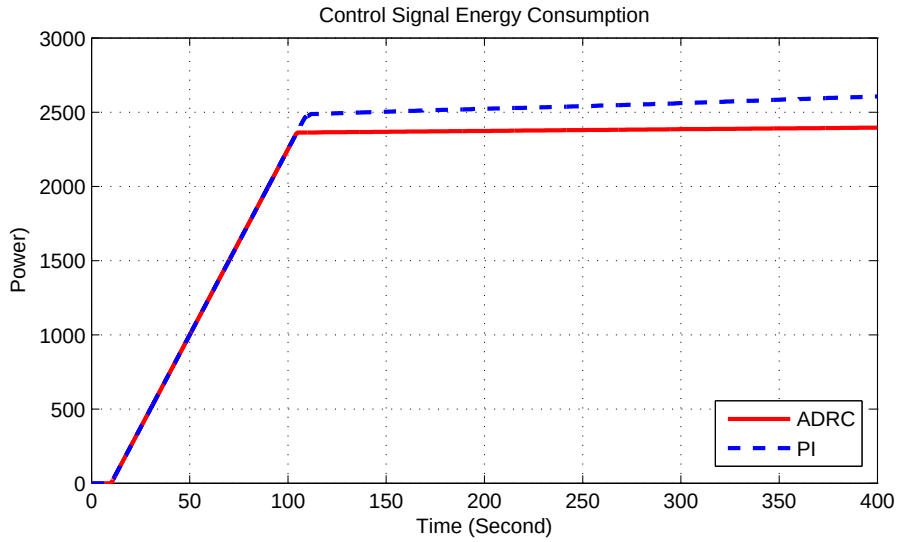

Figure 5.13: Controller Energy Consumption of Real System Pressure Tracking

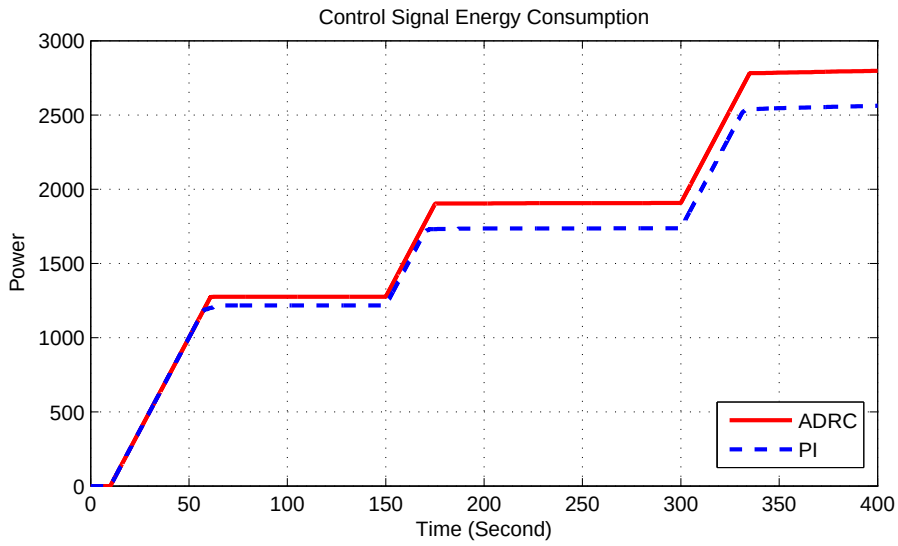

Figure 5.14: Controller Energy Consumption of Multiple Steps Reference Pressure Tracking

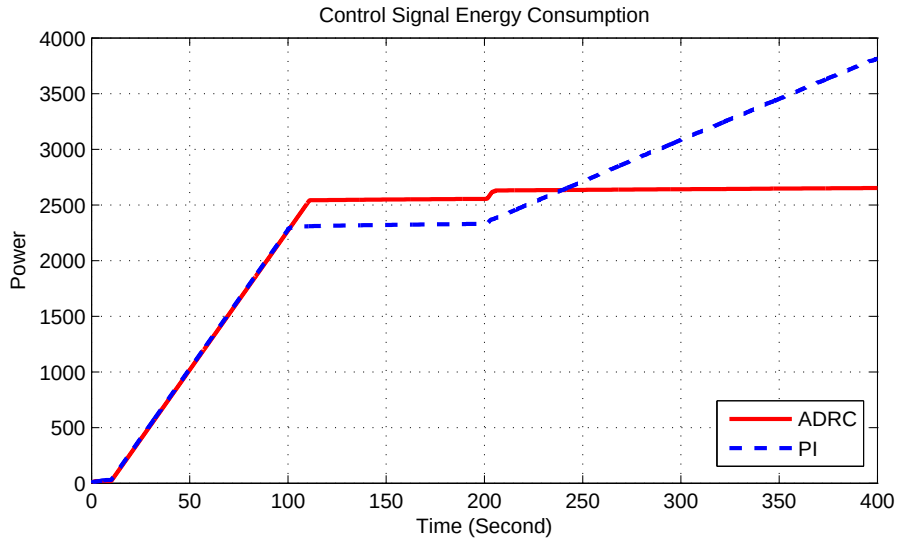

Figure 5.15: Controller Energy Consumption of Real System Pressure Tracking with Disturbance

CHAPTER VI

CONCLUSION AND FUTURE WORK

6.1 Conclusion

The purpose of this research is to perform a simulation and an experimental study of two competing, general purpose industrial control solutions: ADRC and PI. To make the studies relevant to engineering practice, they are performed for a common air pressure control system to regulate the pressure in a tank by using the flow valve, in the presence of leakage, temperature change and components variations. These are all too common in the engineering practice but not systematically studies in terms of controller selection.

To understand the nature of the problem and to carryout the simulation study, the dynamics of the pressure system is studied and the mathematical model is established, based on which a simulation model is constructed. Then, the PI and ADRC control strategies are introduced and implemented in both simulation and hardware. A set of practical scenarios are used for the study, including the set point tracking, the internal disturbance rejection, the external disturbance rejection, and the energy consumption. Based on the results from both the simulation and the experi-

mental studies, as well as the ease of use, it can be concluded that the ADRC is capable to break the monopoly PID in this particular class of industrial control problems. In particular, we draw the following conclusions:

First of all, simple implementation is the main benefits of the PI design, but its parameter tuning is cumbersome. In this research, the mathematic model of the process are used to guide the PI and ADRC tuning but, as shown above, it is much more straightforward to understand how ADRC is tuned. And this removes a major road block in control engineering.

Secondly, from the comparison of the tracking performance in the simulation and experiment results, we show both ADRC and PID meet the requirement needs. In addition, the experiment shows that the same tuning parameters of the ADRC can work in a wider range of set point than the PI control.

Thirdly, the ability of disturbance rejection shows how robust and strong the controller is in the face of adversities. The ADRC holds an absolute advantage over PI in term of disturbance rejection in both simulation and experiment results.

Finally, the energy efficiency is another important factor in the controller selection in industry. The experimental tests demonstrate that ADRC is more energy efficient than PI.

In summary, from the view of controller parameter tuning, the tracking performance, the disturbance rejection capability and the energy consumption, this research shows that ADRC is generally a better solution than PI and is capable of becoming a default solution for industrial control, in place of the time-tested PID solutions.

6.2 Future Research

The future work may include implementing the ADRC controllers in distributed control system (DCS), programmable logic controllers (PLCs) or other forms of digital control to further validate

the conclusions from this thesis. This can be done starting with the the PLC lab at CSU which is quite similar to what is being used in industry. For the air pressure control system, the back pressure regulator can be replaced with a pneumatic valve to make the system multi–variable like many process control problems. The most common process control system in the industry typically controls a combination of process variables, such as both pressure and flow. Two valves produce a multi–input and multi–output system, which will make the research more challenging and practical.

BIBLIOGRAPHY

[1] Z. Gao, "On the centrality of disturbance rejection in automatic control," *ISA Transactions*, vol. 53, pp. 850–857, 2014.

[2] "The Chinese South-Pointing Chariot," Internet: www.ihup.edu/dsimanek/make-chinese/southpointingcarriage.htm, [Dec. 7, 2016].

[3] C. E. Long, J. D. Miles, C. E. Holland, and E. P. Gatzke, "A flexible multivariable experimental air tank system for process control education," *in Proc. American Control Conference*, vol. 1, pp. 688–693, 2003.

[4] J. G. Balchen and K. I. Mumme, *Process Control: Structures and Applications*. Springer, 1987 ed., 1987.

[5] T. E. Marlin, *Process Control: Designing Processes and Control Systems for Dynamic Performance*. McGraw Hill, 2nd ed., 2000.

[6] B. A. Ogunnaike and W. H. Ray, *Process Dynamics, Modeling, and Control*. Oxford University Press, 2nd ed., 1994.

[7] K. J. Astrom and B. Wittenmark, *Computer Controlled Systems: Theory and Design*. Prentice Hall, Inc, 3rd ed., 1997.

[8] B. W. Bequette, *Process Control: Modeling, Design, and Simulation*. Prentice Hall, Inc, 2nd ed., 2003.

[9] J. B. Riggs, *Chemical Process Control*. Ferret Publishing, 2nd ed., 2001.

[10] D. E. Seborg, T. E. Edgar, and D. A. Mellichamp, *Process Dynamics and Control*. John Wiley and Sons Inc, 2nd ed., 1989.

[11] M. Shiee, K. A. Sharifi, M. Fathi, and F. Najafi, "Air pressure vontrol via sliding mode approach using an on/off solenoid valve," *Iranian Conference on Electrical Engineering*, pp. 857–861, 2012.

[12] W. Jian and C. Wenjian, "Development of an adaptive neuro fuzzy method for supply air pressure control in HVAC system," *Systems, Man, and Cybernetics, IEEE International Conference on*, vol. 5, pp. 3806–3809, 2000.

[13] H. Jianjun, T. Qianyuan, B. Yunpeng, and X. Degang, "Constrained generalized predictive control strategy for three level air tank pressure system," *Chinese Control and Decision Conference*, pp. 404–409, 2015.

[14] L. Cheng, W. Wang, A. Aitouche, and Z. Peng, "Robustness evaluation of real time fuzzy logic control of the VGT and EGR on a diesel engine," *Mediterranean Conference on Control and Automation*, pp. 211–217, 2015.

[15] C. Knospe, "PID control," *IEEE Control Systems Magazine*, vol. 26, pp. 30–31, 2006.

[16] Z. Li, "Fuzzy immune PID neural network control method based on boiler steam pressure system," *Pacific-Asia Conference on Circuits, Communications and System*, pp. 1–5, 2011.

[17] W. Tan, Y. Hao, and D. Li, "Design of the PID controller for circulating fluidized bed boiler combustion system," *in Proc. Chinese Control Conference*, 2012.

[18] I. Park, S. Hong, and M. Sunwoo, "Robust air-to-fuel ratio and boost pressure controller design for the EGR and VGT systems using quantitative feedback theory," *IEEE Transactions on Control Systems Technology*, vol. 22, pp. 2218–2231, 2014.

[19] D. Wang, K. Wang, and M. Deng, "The application study of intelligent PlD algorithm for the internal combustion engine control system," *IEEE International Conference on Mechatronics and Automation*, pp. 923–927, 2010.

[20] L. P. Das, S. Paul, and P. K. Roy, "Automatic generation control of an interconnected hydro-thermal system using chemical reaction optimization," *Michael Faraday IET International*, pp. 443–448, 2015.

[21] J. Ziegler and N. Nichols, "Optimal settings for automatic controllers," *Trans. ASME*, vol. 64, pp. 759–768, 1942.

[22] S. ANUSHA, G. KARPAGAM, and E. BHUVANESWARI, "Comparison of tuning methods of PID controller," *International Journal of Management, Information Technology and Engineering*, vol. 2, pp. 1–8, 2014.

[23] P. Rohilla, V. Kumar, and B. Nakra, "Investigation of intelligent control system for non-linear real time pressure control system," *International Journal of Advanced Computer Research*, vol. 5, pp. 212–219, 2015.

[24] K. Astrom and T. Hagglund, "Revisiting the ziegler-nichols step response method for PID control," *International Journal of process Control*, vol. 14, pp. 635–650, 2004.

[25] K. Astrom, O. Garpinger, and T. Hagglund, "Performance and robustness trade-offs in PID control," *International Journal of process Control*, pp. 568–577, 2014.

[26] N. Hambali, M. N. K. Zaki, and A. A. Ishak, "Reformulated tangent method of various PID

controller tuning for air pressure control," *IEEE International Conference on Control System, Computing and Engineering*, pp. 17–22, 2012.

[27] M. Liermann, "PID tuning rule for pressure control applications," *International Journal of Fluid Power*, vol. 14, pp. 7–15, 2013.

[28] Z. Gao, "Active disturbance rejection control from an enduring idea to an emerging technology," *in Proc. International Workshop on Robot Motion and Control, Poznan University of Technology*, pp. 269–282, 2015.

[29] A. Dwyer, "PI and PID controller tuning rules: an overview and personal perspective," *in Proc. IET Irish Signals and Systems Conference*, pp. 161–166, 2006.

[30] A. Dwyer, *Handbook of PI and PID controller tuning rules*. Imperial College Press, 1st ed., 2003.

[31] J. Han, "Control theory: Model approach or control approach," *Syst. Sci. Math*, vol. 9, pp. 328–335, 1989.

[32] J. Han and W. Wang, "Nonlinear tracking-differentiator," *Syst. Sci. Math*, vol. 14, pp. 177–183, 1994.

[33] J. Han, "Nonlinear PID controller," *J. Autom*, vol. 20, pp. 487–490, 1994.

[34] J. Han, "Extended state observer for a class of uncertain plants," *Control Decis*, vol. 10, pp. 85–88, 1995.

[35] J. Han, "From PID to active disturbances rejection control," *Syst. Sci. Math*, vol. 9, pp. 13–18, 2002.

[36] J. Han, "Active disturbances rejection control technique," *Frontier Sci.*, vol. 1, pp. 24–31, 2007.

[37] J. Han, “From PID to active disturbances rejection control,” *IEEE Transactions on Industrial Electronics*, vol. 56, pp. 900–906, 2009.

[38] Z. Gao, “Scaling and bandwidth-parameterization based controller tuning,” *American Control Conference*, vol. 6, pp. 4989–4996, 2003.

[39] G. Tian and Z. Gao, “Benchmark tests of active disturbance rejection control on an industrial motion control platform,” *in Proc. American Control Conference*, pp. 5552–5557, 2009.

[40] Q. Zheng and Z. Gao, “An energy saving, factory-validated disturbance decoupling control design for extrusion processes,” *in Proc. IEEE World Congress on Intelligent Control and Automation*, pp. 2891–2896, 2012.

[41] “Technical Reference Manual, TMS320F28069M, TMS320F28068M InstaSPINâĎć-MOTION Software,” Literature Number: SPRUHJ0A. Texas Instruments. Revised Nov, 2013.

[42] “Kinetis Motor Suite, Freescale Semiconductor Inc,” Internet: http://cache.freescale.com/files/soft-dev-tools/doc/fact-sheet/KINTMOTSUITFS.pdf, [June 2015].

[43] “Ohioepolymer News, LineStream Technologies: Advanced Control, Made Simple,” Internet: http://www.polymerohio.org/index.php, [Oct. 2016].

[44] “LineStream Technologies signs licensing deal with Texas Instruments,” The Plain Dealer, July 12th, 2011.

[45] “LineStream Technologies 5 Million Investment Timed Perfectly,” Crain’s Cleveland Business, Mar, 2012.

[46] “Control Freaks,” Inside Business Magazine, November-December Issue, 2011.

[47] "Look Ahead," Cutting Tool Engineering, January, 2009.

[48] "A New Industrial Revolution," The Plain Dealer, Sept. 2nd, 2008.

[49] "Say You Want a Machine Control Revolution," Industry Week, Oct, 2008.

[50] "First CSU Commercialization Effort Helps Manufacturers Fine-tune Machinery," Crain's Cleveland Business, Aug, 2008.

[51] S. Yang, H. Xie, K. Song, X. Li, and Z. Gao, "On boost pressure control of diesel engines with double-layer passage turbocharger," *Society of Instrument and Control Engineers of Japan (SICE)*, pp. 498–503, 2015.

[52] W. Xue, W. Bai, S. Yang, K. Song, Y. Huang, and H. Xie, "ADRC with adaptive extended state observer and its application to air fuel ratio control in gasoline engines," *IEEE Transactions on Industrial Electronics*, vol. 62, pp. 5847–5857, 2015.

[53] Y. He, Y. Yan, H. Xie, and Z. Gao, "ADRC for variable valve timing system of gasoline engine," *Chinese Control Conference*, vol. 9, pp. 6305–6309, 2011.

[54] F. Pan, Q. Liu, L. Sun, D. Li, and W. Tan, "A novel design of active disturbance rejection controller and its application in the circulating fluidized bed boiler combustion system," *American Control Conference*, pp. 3950–3955, 2015.

[55] Z. Ruiqing, M. Liangyu, M. Yongguang, and W. Bingshu, "Active disturbance rejection control of once-through boiler unit coordinated system based on pseudo-diagonalization,"

[56] S. Zhao and Z. Gao, "An active disturbance rejection based approach to vibration suppression in two-inertia systems," *Asian Journal of Control*, vol. 15, pp. 350–362, 2013.

[57] Q. Zheng and Z. Gao, "On active disturbance rejection for systems with input time-delays and unknown dynamics," *American Control Conference*, pp. 95–100, 2016.

[58] M. J. Jankovic, “Introduction to modeling and control of internal combustion engine systems,” *IEEE Control Systems*, pp. 96–99, 2005.

[59] J. C. Maxwell, “On governors,” *Proceedings of Royal Society*, p. 100, 1868.

[60] Bennett and Stuart, “Nicholas minorsky and the automatic steering of ships,” *IEEE Control Systems Magazine*, pp. 10–15, 1984.